

# High net CO<sub>2</sub> and CH<sub>4</sub> release at a eutrophic shallow lake on a formerly drained fen

D. Franz<sup>1</sup>, F. Koebsch<sup>1</sup>, E. Larmanou<sup>1</sup>, J. Augustin<sup>2</sup> and T. Sachs<sup>1</sup>

[1] {Helmholtz Centre Potsdam, GFZ German Research Centre for Geosciences, Telegrafenberg, 14473 Potsdam, Germany}

[2] {Institute for Landscape Biogeochemistry, Leibniz Centre for Agricultural Landscape Research (ZALF), Eberswalder Str. 84, 15374 Müncheberg, Germany}

Correspondence to: D. Franz (daniela.franz@gfz-potsdam.de)

## Abstract

Drained peatlands often act as carbon dioxide (CO<sub>2</sub>) hotspots. Raising the groundwater table is expected to reduce their CO<sub>2</sub> contribution to the atmosphere and revitalize their function as carbon (C) sink in the long term. Without strict water management rewetting often results in partial flooding and the formation of spatially heterogeneous, nutrient-rich shallow lakes. Uncertainties remain as to when the intended effect of rewetting is achieved, as this specific ecosystem type has hardly been investigated in terms of greenhouse gas (GHG) exchange. In most cases of rewetting, methane (CH<sub>4</sub>) emissions increase under anoxic conditions due to a higher water table and in terms of global warming potential (GWP) outperform the shift towards CO<sub>2</sub> uptake, at least in the short-term.

Based on eddy covariance measurements we studied the ecosystem–atmosphere exchange of CH<sub>4</sub> and CO<sub>2</sub> at a shallow lake situated on a former fen grassland in Northeast (NE) Germany. The lake evolved shortly after flooding, 9 years previous to our investigation period. The ecosystem consists of two main surface types: open water (inhabited by submerged and floating vegetation) and emergent vegetation (particularly including the eulittoral zone of the lake, dominated by *Typha latifolia*). To determine the individual contribution of the two main surface types to the net CO<sub>2</sub> and CH<sub>4</sub> exchange of the whole lake ecosystem, we combined footprint analysis with CH<sub>4</sub> modelling and net ecosystem exchange (NEE) partitioning.

The CH<sub>4</sub> and CO<sub>2</sub> dynamics were strikingly different between open water and emergent vegetation. Net CH<sub>4</sub> emissions from the open water area were around 4-fold higher than from emergent vegetation stands, accounting for 53 and 13 g CH<sub>4</sub> m<sup>-2</sup> a<sup>-1</sup>, respectively. In addition, both surface types were net CO<sub>2</sub> sources with 158 and 750 g CO<sub>2</sub> m<sup>-2</sup> a<sup>-1</sup>, respectively. Unusual meteorological conditions in terms

32 of a warm and dry summer and a mild winter might have facilitated high respiration rates. In sum, even  
33 after 9 years of rewetting the lake ecosystem exhibited a considerable C loss and global warming  
34 impact, the latter mainly driven by high CH<sub>4</sub> emissions. We assume the eutrophic conditions in  
35 combination with permanent high inundation as major reasons for the unfavourable GHG balance.

36

## 37 **1 Introduction**

38 Peatland ecosystems play an important role in global greenhouse gas (GHG) cycles, although they  
39 cover only about 3 % of the earth's surface (Frolking et al. 2011). Peat growth depends on the  
40 proportion of carbon (C) sequestration and release. Pristine peatlands act as long-term C sinks and are  
41 near-neutral (slightly cooling) regarding their global warming potential (GWP; Frolking et al. 2011),  
42 dependent on rates of C sequestration and methane (CH<sub>4</sub>) emissions. However, many peatlands  
43 worldwide are used e.g. for agriculture, as are more than 85% of the peatlands in Germany and the  
44 Netherlands (Silvius et al. 2008). Drainage is associated with shrinkage and internal phosphor  
45 fertilisation of the peat (Zak et al. 2008). Moreover, the hydrology of the area as well as physical and  
46 chemical peat characteristics are changing (Holden et al. 2004, Zak et al. 2008). Above all, drained and  
47 intensively managed peatlands are known as strong sources of carbon dioxide (CO<sub>2</sub>; e.g. Joosten et al.  
48 2010, Hatala et al. 2012, Beetz et al. 2013). On the other hand, lowering the water table is typically  
49 accompanied with decreasing CH<sub>4</sub> emissions (Roulet et al. 1993). Emission factors of 1.6 g CH<sub>4</sub> m<sup>-2</sup> a<sup>-1</sup>  
50 and 2235 g CO<sub>2</sub> m<sup>-2</sup> a<sup>-1</sup> were assigned to temperate deep-drained nutrient-rich grassland in the 2013  
51 wetland supplement to the 2006 IPCC Guidelines for National Greenhouse Gas Inventories (IPCC 2014).

52 In the last decades rewetting of peatlands attracted attention in order to stop soil degradation, reduce  
53 CO<sub>2</sub> emissions and to recover their functions as C and nutrient sink and ecological habitat (Zak et al.  
54 2015). Large rewetting projects were initiated, e.g. the Mire Restoration Program of the federal state  
55 of Mecklenburg-West Pomerania in Northeast (NE) Germany (Berg et al. 2000) starting in 2000 and  
56 involving 20 000 ha of formerly drained peatlands, thereby especially fens (Zerbe et al. 2013) e.g. in  
57 the Peene river catchment. However, uncertainties remain as to when the intended effects of  
58 rewetting are achieved. Only few studies exist on the temporal development of GHG emissions of  
59 rewetted fens, especially on longer time scales. Augustin and Joosten (2007) discuss three very  
60 different states following peatland rewetting based on observations at Belarusian mires, though  
61 without specifying the individual lengths of the phases. Broad agreement exists concerning the CH<sub>4</sub>  
62 hot spot characteristic of newly rewetted peatlands (e.g. Meyer et al. 2001, Hahn-Schöfl et al. 2011,  
63 Knox et al. 2015). However, a rapid recovery of the net CO<sub>2</sub> sink function is not consistently reported  
64 (e.g. Wilson et al. 2007).

65 Peatlands develop a distinct microtopography after drainage and subsequent subsidence. Rewetting  
66 e.g. in the Peene river catchment resulted in the formation of large-scale shallow lakes in the lower  
67 parts of the fens, with water depths usually below 1 m (Zak et al. 2015, Steffenhagen et al. 2012). These  
68 new ecosystems are nutrient-rich and most often strikingly different from natural peatlands. They  
69 experience a rapid secondary plant succession (Zak et al. 2015). Helophytes are expected to  
70 progressively enter the open water body over the time leading to the terrestrialisation of the shallow  
71 lake and in the best case peat formation. However, this new ecosystem type and its progressive  
72 transformation have hardly been investigated in terms of GHG dynamics. The ecosystem-inherent  
73 spatial heterogeneity suggests complex patterns of GHG emissions due to distinct GHG source or sink  
74 characteristics of the involved surface types (generally open water and the littoral zone) resulting in  
75 measurement challenges. Site-specific heterogeneity implicitly has to be considered for the evaluation  
76 of ecosystem scale flux measurements (e.g. Barcza et al. 2009, Hendriks et al. 2010, Herbst et al. 2011,  
77 Hatala Matthes et al. 2014). The importance of small open water bodies in wetlands as considerable  
78 GHG sources was highlighted in previous studies (e.g. by Schrier-Uijl et al. 2011, Zhu et al. 2012, IPCC  
79 2014) and in case of CH<sub>4</sub> even for landscape-scale budgets e.g. by Repo et al. (2007). In addition, the  
80 littoral zone of lakes is often found to be a CH<sub>4</sub> hot spot (Juutinen et al. 2003, Wang et al. 2006) with a  
81 contribution of up to 90 % to the whole-lake CH<sub>4</sub> release (Smith and Lewis 1992), albeit depending on  
82 the lake size (Bastviken et al. 2004) and plant community. Rööm et al. (2014) measured the largest CH<sub>4</sub>  
83 (and CO<sub>2</sub>) emissions of a temperate eutrophic lake at the helophyte zone within the littoral.

84 The objectives of this study are 1) to investigate the ecosystem-atmosphere exchange of CH<sub>4</sub> and CO<sub>2</sub>  
85 (NEE) of a nutrient-rich lake ecosystem emerged at a former fen grassland and 2) particularly infer the  
86 individual GHG dynamics of the main surface types within the ecosystem and quantify their  
87 contribution to the annual exchange rates. Therefore, we applied the eddy covariance technique from  
88 May 2013 to May 2014 and used an analytical footprint model to downscale the spatially integrated,  
89 half-hourly fluxes to the main surface types “open water” and “emergent vegetation”. The resulting  
90 source area (i.e. spatial origin of the flux) fractions were then included in a temperature response (CH<sub>4</sub>)  
91 and NEE partitioning model (CO<sub>2</sub>) in order to quantify the source strength of the two surface types.

92

## 93 **2 Material and methods**

### 94 **2.1 Study site**

95 The study site “Polder Zarnekow” is a rewetted, rich fen (minerotrophic peatland) located in the Peene  
96 river valley (Mecklenburg-West Pomerania, NE Germany, 53°52.5′ N 12°53.3′ E, see Fig. 1), with less  
97 than 0.5 m a.s.l. elevation. It is part of the Terrestrial Environmental Observatories Network (TERENO).

98 The temperate climate is characterised by a long-term mean annual air temperature and mean annual  
99 precipitation of 8.7 °C and 584 mm, respectively (German Weather Service, meteorological station  
100 Teterow, 24 km SW of the study site; reference period 1981–2010). The geomorphological character  
101 of the area is predominantly a result of the Weichselian glaciation as the last period of the Pleistocene  
102 (Steffenhagen et al. 2012). The fen developed with continuous percolating groundwater flow (Succow  
103 2001). Peat depth partially reaches 10 m (Hahn-Schöfl et al. 2011). Drainage was initialized in the 18<sup>th</sup>  
104 century and strongly intensified between 1960 and 1990 within an extensive melioration program  
105 (Höper et al. 2008). The decline of the water table to > 1 m below surface and subsequent  
106 decomposition and mineralisation of the peat (especially in the upper 30 cm, Hahn-Schöfl et al. 2011)  
107 caused phosphor fertilisation (Zak et al. 2008) and soil subsidence to levels below that of adjacent  
108 freshwater bodies (Steffenhagen et al. 2012, Zerbe et al. 2013). The latter simplified the rewetting  
109 process which was initiated in winter 2004/2005 by opening the dikes.

110 In consequence of flooding the drained fen was converted into a spatially heterogeneous site of  
111 emergent vegetation (on temporarily inundated soil) and permanent open water areas. In this study  
112 we focus on a eutrophic and polymictic lake (open water body about 7.5 ha) as part of the rewetted  
113 area, with water depths ranging from 0.2 to 1.2 m (2004 to 2012; Zak et al. 2015). During the study  
114 period the open water body of the lake was inhabited by submerged and floating macrophytes,  
115 particularly *Ceratophyllum demersum*, *Lemna minor*, *Spirodela polyrhiza* (Steffenhagen et al. 2012) and  
116 *Polygonum amphibium*, which rather corresponds to the sublittoral zone in a typical lake zonation.  
117 *Ceratophyllum* and *Lemna* sp. were already reported to colonise the lake in the second year of  
118 rewetting (Hahn-Schöfl et al. 2011). *Phalaris arundinacea*, that dominated the fen before rewetting,  
119 died off in the first year of inundation (Hahn-Schöfl et al. 2011) and has been limited to the non-  
120 inundated periphery of the ecosystem. Helophytes (e.g. *Glyceria*, *Typha*) started the colonisation of  
121 lake margins and other temporarily inundated areas in the third year of rewetting. The eulittoral zone  
122 of the lake is now dominated by *Typha latifolia* stands gradually colonising the open water in the last  
123 years. Emergent vegetation stands also include sedges as *Carex gracilis* (Steffenhagen et al. 2012). At  
124 the bottom of the shallow lake an up to 30 cm thick layer of organic sediment evolved, initially fed by  
125 fresh plant material of the former vegetation and since then continuously replenished by recent  
126 aquatic plants and helophytes after die-back (Hahn-Schöfl et al. 2011).

## 127 **2.2 Eddy covariance and additional measurements**

128 We conducted eddy covariance (EC) measurements of CO<sub>2</sub> and CH<sub>4</sub> exchange on a tower placed on a  
129 stationary platform at the NE edge of the shallow lake (see Fig. 1). Thereby we ensured to frequently  
130 catch the signal from both the open water body and the *Typha latifolia* dominated belt of the shallow  
131 lake (eulittoral zone). We defined an area of interest (AOI) in order to focus on an ecosystem

132 dominated by a shallow lake and to avoid a possible impact of the farm and grassland to the north of  
 133 the shallow lake. The EC measurement setup included: an ultrasonic anemometer for the 3D wind  
 134 vector ( $u$ ,  $v$ ,  $w$ ) and sonic temperature (HS-50, Gill, Lymington, Hampshire, UK), an enclosed-path  
 135 infrared gas analyser (IRGA) and an open-path IRGA for CO<sub>2</sub>/H<sub>2</sub>O and CH<sub>4</sub> concentrations, respectively  
 136 (LI-7200 and LI-7700, LI-COR Biogeosciences, Lincoln NE, USA). Flowrate was about 10-11 l min<sup>-1</sup>.  
 137 Measurement height was on average 2.63 m above the water surface at the position of the tower,  
 138 depending on the water level. We recorded raw turbulence and concentration data with a LI-7550  
 139 digital data logger system (LI-COR Biogeosciences, Lincoln NE, USA) at 20 Hz in half-hourly files. The  
 140 dataset is shown in Coordinated Universal Time (UTC), which is 1 hour behind local time (LT).

141 We further equipped the tower with instrumentation for net radiation, air temperature/humidity, 2D  
 142 wind direction and speed, incoming and reflected photosynthetic photon flux density (PPFD/PPFD<sub>r</sub>)  
 143 and water level. Additional measurements in close proximity to the tower included precipitation, soil  
 144 heat flux as well as soil and water temperature. Soil temperature was measured below the water  
 145 column in depths of 10 cm, 20 cm, 30 cm, 40 cm and 50 cm and water temperature at the sediment-  
 146 water-interface. All non-eddy covariance-related measurements were logged as 1 min averages/sums  
 147 (precipitation). Gaps were filled with measurements of the Leibniz Centre for Agricultural Landscape  
 148 Research (ZALF, Müncheberg, Germany) at the same platform and a nearby climate station (Climate  
 149 station Karlshof, GFZ German Research Centre for Geosciences, 14 km distance from study site, Itzerott  
 150 2015).

151 A water density gradient was calculated based on the temperature at the water surface and at the  
 152 sediment-water interface. The water surface temperature was calculated based on the Stefan-  
 153 Boltzmann law (see e.g. Foken et al. 2008):

$$154 \quad T_w = \sqrt[4]{\frac{I}{\varepsilon_w \sigma_{SB}}} \quad (1)$$

155

156 where  $T_w$  is the water surface temperature (K),  $I$  is the long-wave outgoing radiation (W m<sup>-2</sup>),  $\varepsilon_w$  is  
 157 the infrared emissivity of water (0.960) and  $\sigma_{SB}$  is the Stefan–Boltzmann constant (5.67·10<sup>-8</sup> W m<sup>-2</sup> K<sup>-4</sup>). We calculated the density of the air-saturated water at the water surface and the sediment-water  
 158 interface according to Bignell (1983):

$$160 \quad \rho_{as} = \rho_{af} - 0.004612 + 0.000106 * T \quad (2)$$

161 where  $\rho_{as}$  is the density of the respective air-saturated water (k m<sup>-3</sup>),  $\rho_{af}$  is the density of the  
 162 respective air-free water (k m<sup>-3</sup>; see Wagner and Pruß 2002) at atmospheric pressure (1013 hPa) and  
 163  $T$  is the respective water temperature (°C). The gradient of the two water densities (air-saturated)

164  $\Delta\rho/\Delta z$  was calculated as difference of the water density (air-saturated) at the sediment-water  
165 interface and the surface water density (air-saturated), divided by the distance (m) between the two  
166 basic temperature measurements. Changes of the distance due to the fluctuating water level were  
167 considered. Positive and negative gradients indicate periods of stratification and thermally induced  
168 convective mixing of the water column, respectively.

### 169 **2.3 Flux computation and further processing**

170 For this analysis we used data from 14 May 2013 to 14 May 2014. We calculated half-hourly fluxes of  
171 CO<sub>2</sub> and CH<sub>4</sub> based on the covariances between the respective scalar concentration and the vertical  
172 wind velocity using the processing package EddyPro 5.2.0 (LI-COR, Lincoln, Nebraska, USA). Sonic  
173 temperature was corrected for humidity effects according to van Dijk et al. (2004). Artificial data spikes  
174 were removed from the 20 Hz data following Vickers and Mahrt (1997). We used the planar fit method  
175 (Finnigan et al. 2003, Wilczak et al. 2001) for axis rotation and defined the sector borders according to  
176 Siebicke et al. (2012). Block averaging was used to detrend turbulent fluctuations. For time lag  
177 compensation we applied covariance maximization (Fan et al. 1990). Spectral losses due to crosswind  
178 and vertical instrument separation were corrected according to Horst and Lenschow (2009). The  
179 methods of Moncrieff et al. (2004) and Fratini et al. (2012) were used for the correction of high-pass  
180 filtering and low-pass filtering effects, respectively. For fluctuations of CH<sub>4</sub> density we corrected  
181 changes in air density according to Webb et al. (1980), considering LI-7700-specific spectroscopic  
182 effects (McDermitt et al. 2011). According to the micrometeorological sign convention, positive values  
183 represent fluxes from the ecosystem into the atmosphere (emission) and negative values fluxes from  
184 the atmosphere into the ecosystem (ecosystem uptake).

### 185 **2.4 Quality assurance**

186 We filtered the averaged fluxes according to their quality as follows (see Table 1, for final measurement  
187 data coverage see Fig. A1):

- 188 - We rejected fluxes with quality flag 2 (QC 2, bad quality) based on the 0-1-2 system of Mauder  
189 and Foken (2004).
- 190 - CH<sub>4</sub> fluxes were skipped if the signal strength (RSSI) was below the threshold of 14 %. This  
191 threshold was estimated according to Dengel et al. (2011).
- 192 - Fluxes with friction velocity ( $u^*$ ) < 0.12 m s<sup>-1</sup> and > 0.76 m s<sup>-1</sup> were not included due to  
193 considerably high fluxes beyond these thresholds, which were estimated similar to the  
194 procedure described in Aubinet et al. (2012) based on binned  $u^*$  classes. The storage term was  
195 calculated as described in Béziat et al. (2009).

196 - Unreasonably high positive and negative fluxes (0.2 %/99.8 % percentile) were discarded from  
197 the CO<sub>2</sub> and CH<sub>4</sub> flux dataset.

198 Quality control (apart from EddyPro internal steps) and the subsequent processing steps were  
199 performed with the free software environment R (R Core Team 2012).

## 200 **2.5 Footprint modelling**

201 We applied footprint analysis to determine the source area including the fractions of the surface types  
202 of each quality-controlled half-hourly flux using a footprint calculation procedure following Göckede  
203 et al. (2004). The source area functions were calculated based on the analytical footprint model of  
204 Kormann and Meixner (2001). Roughness length and vegetation height were estimated with an  
205 iterative algorithm (see also Barcza et al. 2009). Based on an aerial image (GoogleEarth,  
206 <http://earth.google.com/>) the surface of our study site was classified into two main types and  
207 implemented in a land cover grid: “open water” including in particular the open water body of the  
208 shallow lake and “emergent vegetation” with a height up to 2 m and including the eulittoral zone of  
209 the shallow lake dominated by *Typha latifolia*. The cumulative annual footprint climatology was  
210 calculated following Chen et al. (2011). Fluxes were excluded where footprint information was not  
211 available or more than 20 % of the source area was outside the AOI (see Fig. 1 and Table 1). The  
212 fractional coverage within the AOI ( $A_i$ ) was 21.7 % for open water.

213 Quasi-continuous source area information for the two surface types were achieved by gapfilling the  
214 results of the footprint model with the means of the source area fractions of the surface types ( $\Omega_i$ ) for  
215 1°-wind direction-intervals, separately for stable and unstable conditions. In case the sum of the  $\Omega_i$  was  
216 less than 100 %, when the source area exceeded the set borders, we assigned the remaining  
217 contribution percentages to emergent vegetation, as the area beyond the borders is dominated by  
218 emergent vegetation rather than open water.

## 219 **2.6 Gapfilling**

220 A Marginal Distribution Sampling (MDS)) approach proposed by Reichstein et al. (2005), available as  
221 web tool based on the R package REddyProc ([http://www.bgc-](http://www.bgc-jena.mpg.de/REddyProc/brew/REddyProc.rhtml)  
222 [jena.mpg.de/REddyProc/brew/REddyProc.rhtml](http://www.bgc-jena.mpg.de/REddyProc/brew/REddyProc.rhtml)) was applied for gapfilling and partitioning of NEE  
223 measurements (MDS<sub>CO<sub>2</sub>nofoot</sub>), with air temperature as temperature variable. For the gapfilling of CH<sub>4</sub>  
224 measurements non-linear regression (NLR) was applied (NLR<sub>CH<sub>4</sub>nofoot</sub>):

$$225 F_{CH_4} = \exp(a + b_1 \cdot X_1 + \dots + b_j \cdot X_j) \quad (3)$$

226 where  $a$  and  $b_1...b_j$  are fitting parameters and  $X_1...X_j$  are environmental parameters. Several  
227 environmental parameters, which were reported to be correlated with CH<sub>4</sub> flux on different time  
228 scales, were tested to find the best bi- or multivariate NLR model for the ecosystem CH<sub>4</sub> flux: pressure  
229 change,  $u^*$ , PAR, air temperature, soil heat flux, soil/peat temperature in different heights and  
230 waterlevel. Only fluxes of the best quality (QC 0) were used to fit the NLR model and the MDS.

## 231 **2.7 Calculation of the annual CO<sub>2</sub> and CH<sub>4</sub> budget and the global warming** 232 **potential (GWP)**

233 We used the continuous flux datasets derived from gapfilling for the calculation of annual CO<sub>2</sub> and CH<sub>4</sub>  
234 budgets. The ecosystem GHG balance was calculated by summation of the net ecosystem exchange of  
235 CO<sub>2</sub> and CH<sub>4</sub> using the global warming potential (GWP) of each gas at the 100-year time horizon (IPCC,  
236 2013). According to the IPCC AR5 (IPCC, 2013) CH<sub>4</sub> has a 28-fold global warming potential compared  
237 to CO<sub>2</sub> (without inclusion of climate-carbon feedbacks).

238 The uncertainty of the annual estimates was calculated as the square root of the sum of the squared  
239 random error (measurement uncertainty) and gapfilling error within the one-year observation period  
240 (see e.g. Hommeltenberg et al. 2014, Shoemaker et al. 2015). An estimation of the random uncertainty  
241 due to the stochastic nature of turbulent sampling according to Finkelstein and Sims (2001) is  
242 implemented in EddyPro 5.2.0. In case of the MDS approach the gapfilling error (standard error) was  
243 calculated from the standard deviation of the fluxes used for gapfilling, provided by the web tool. For  
244 budgets based on the NLR approach we used the residual standard error of the NLR model as gapfilling  
245 error (following Shoemaker et al. 2001).

## 246 **2.8 Estimation of surface type fluxes**

247 To estimate the specific surface type fluxes, we combined footprint analysis with NEE partitioning  
248 (using NLR) to assign gross primary production (GPP) and ecosystem respiration ( $R_{eco}$ ) to the two main  
249 surface types (NLR<sub>CO2foot</sub>).  $R_{eco}$  and GPP were modelled as sum of the two surface type fluxes weighted  
250 by  $\Omega_i$  (analogous to Forbrich et al. 2011). Night-time  $R_{eco}$  (global radiation < 10 W m<sup>-2</sup>) was estimated  
251 by the exponential temperature response model of Lloyd and Taylor (1994) assuming that night-time  
252 NEE represents the night-time  $R_{eco}$ :

$$253 R_{eco} = \sum_{i=1}^2 \Omega_i \cdot R_{ref_i} \cdot \exp\left(E_{0_i} \left( \frac{1}{T_{ref} - T_0} - \frac{1}{T_{air} - T_0} \right)\right) \quad (4)$$

254 where  $R_{eco}$  is the half-hourly measured ecosystem respiration ( $\mu\text{mol}^{-1}\text{m}^{-2}\text{s}^{-1}$ ),  $\Omega_i$  is the source area  
255 fraction of the respective surface type,  $R_{ref}$  is the respiration rate at the reference temperature  $T_{ref}$   
256 (283.15 K),  $E_0$  defines the temperature sensitivity,  $T_0$  is the starting temperature constant (227.13 K)



257 and  $T_{air}$  the mean air temperature during the flux measurement. The model parameters achieved for  
 258 night-time  $R_{eco}$  were applied for the modelling of day-time  $R_{eco}$ . GPP was calculated by subtracting day-  
 259 time  $R_{eco}$  from the measured NEE. GPP was further modelled using a rectangular, hyperbolic light  
 260 response equation based on the Michaelis–Menten kinetic (see e.g. Falge et al. 2001):

$$261 \quad GPP = \sum_{i=1}^2 \Omega_i \cdot \left( \frac{GP_{max_i} \cdot \alpha_i \cdot PAR}{\alpha_i \cdot PAR + GP_{max_i}} \right) \quad (5)$$

262 where  $GPP$  is the calculated gross primary production ( $\mu\text{mol}^{-1}\text{m}^{-2}\text{s}^{-1}$ ),  $\Omega_i$  is the source area fraction  
 263 of the respective surface type,  $GP_{max}$  is the maximum C fixation rate at infinite photon flux density of  
 264 the photosynthetic active radiation  $PAR$  ( $\mu\text{mol}^{-1}\text{m}^{-2}\text{s}^{-1}$ ),  $\alpha$  is the light use efficiency ( $\text{mol CO}_2 \text{ mol}^{-1}$   
 265 photons). We calculated one parameter set for  $R_{eco}$  and GPP per day based on a moving window of 28  
 266 days. In order to avoid over-parameterization we introduced fixed values of 150 for  $E_0$  and -0.03 and -  
 267 0.01 for  $\alpha$  of emergent vegetation and water bodies, respectively, to get reasonable parameter values  
 268 for  $R_{ref}$  and  $GP_{max}$ . We excluded parameter sets for  $R_{eco}$  or GPP, if one of the two  $R_{ref}$  and  $GP_{max}$   
 269 parameter values was insignificant ( $p\text{-value} \geq 0.05$ ), negative or zero. In addition, the 1 %/99 %  
 270 percentiles of  $GP_{max}$  were excluded. These gaps within the parameter set were filled by linear  
 271 interpolation. Gaps remained in  $R_{eco}$  and GPP time series due to gaps in the environmental variables.  
 272 Gaps up to 3 hours length were filled by linear interpolation. Larger gaps were filled with the mean of  
 273 the flux during the same time of the day before and after the gap. Due to the moving window approach,  
 274 we could not estimate model parameters for the first and last 14 days of our study period. Instead, we  
 275 applied the first and last estimated parameter set, respectively. Modelled GPP and  $R_{eco}$  were summed  
 276 up to half-hourly NEE fluxes and used for alternative NEE gapfilling ( $NLR_{CO2foot}$ ).

277 As for NEE we expect different  $\text{CH}_4$  emission rates of the two surface types. Thus, we extended the NLR  
 278 model ( $NLR_{CH4nofoot}$ ) in a way that the  $\text{CH}_4$  flux is the sum of the two surface type fluxes weighted by  $\Omega_i$   
 279 ( $NLR_{CH4foot}$ ):

$$280 \quad F_{CH_4} = \sum_{i=1}^2 \Omega_i \cdot \exp(a_i + b_{1i} \cdot X_1 + \dots + b_{ji} \cdot X_j) \quad (6)$$

281 where  $\Omega_1$  is the source area fraction of the respective surface type. Considering the principle of  
 282 parsimony, we combined up to three parameters besides the contribution of the surface types.  
 283 Remaining gaps were filled by interpolation. Surface type  $\text{CO}_2$  and  $\text{CH}_4$  fluxes were derived based on  
 284 the fitted NLR parameters.

285 We calculated the annual budgets of  $\text{CO}_2$  and  $\text{CH}_4$  for the EC source area, the surface types (assuming  
 286 source area fraction of 100 % for the respective surface type) and the AOI, the latter following Forbrich  
 287 et al. (2011) by applying Eq. 4 and Eq. 5 for  $\text{CO}_2$  as well as Eq. 6 for  $\text{CH}_4$  with the fitted parameters, but

288  $A_i$  instead of  $\Omega_i$  as weighting surface type contribution. The gapfilling error for the  $NLR_{CO_2foot}$  model was  
289 based on the residual standard error of both  $R_{eco}$  and GPP.

290

## 291 **3 Results**

### 292 **3.1 Environmental conditions and fluxes of CO<sub>2</sub> and CH<sub>4</sub>**

293 Mean annual air temperature and annual precipitation for the study period were 10.1 °C and 416.5  
294 mm, respectively, indicating an unusual dry and warm measurement period compared to the long-  
295 term average. The summer 2013 was among the 10 warmest since the beginning of the measurements  
296 in 1881 (German Weather Service DWD). From June to August monthly averaged air temperature was  
297 0.2 up to 0.9 °C higher and precipitation was 9.1 up to 38.1 mm less than the long-term averages. The  
298 open water area of the shallow lake was densely vegetated with submerged and floating macrophytes.  
299 A summertime algae slick accumulated in the NE part of the shallow lake. Winter 2013/2014 was  
300 characterised by exceptionally mild temperatures and very sparse precipitation. However, a short cold  
301 period (see Fig. 2) resulted in ice cover on the shallow lake between 21 January and 16 February 2014.  
302 The water level of the shallow lake fluctuated between 0.36 and 0.77 m (at the position of the sensor)  
303 and had its minimum at the end of August/beginning of September and its maximum in January. We  
304 observed the exposure of normally inundated soil surface at emergent vegetation stands during the  
305 dry period in summer 2013.

306 Both CO<sub>2</sub> and CH<sub>4</sub> flux measurement time series showed a clear seasonal trend with a median CO<sub>2</sub> flux  
307 of 0.57  $\mu\text{mol m}^{-2} \text{s}^{-1}$  and a median CH<sub>4</sub> flux of 0.02  $\mu\text{mol m}^{-2} \text{s}^{-1}$ . CH<sub>4</sub> emissions peaked in mid-August  
308 2013 with 0.57  $\mu\text{mol m}^{-2} \text{s}^{-1}$ . The highest net CO<sub>2</sub> uptake ( $-15.34 \mu\text{mol m}^{-2} \text{s}^{-1}$ ) and release (21.04  $\mu\text{mol}$   
309  $\text{m}^{-2} \text{s}^{-1}$ ) were both observed in June 2013. To investigate the potential presence of a diurnal cycle of  
310 CO<sub>2</sub> and CH<sub>4</sub> fluxes throughout the study period we normalised the mean half-hourly CO<sub>2</sub> and CH<sub>4</sub>  
311 fluxes per month with the respective minimum/ maximum and median of the half-hourly fluxes of the  
312 specific month (modified from Rinne et al. 2007). A pronounced diurnal cycle of CO<sub>2</sub> fluxes with peak  
313 uptake around midday and peak release around midnight was obvious until November 2013 and  
314 beginning in March 2014 (see Fig. 3), although less pronounced in these two months. We found a clear  
315 diurnal cycle of CH<sub>4</sub> fluxes from June to September 2013 and in March 2014 (April 2014 based on 3  
316 days only and May 2014 not available as the sensor was dismantled) with daily peaks during night-time  
317 (around midnight until early morning). The water density gradient indicates thermally induced  
318 convective mixing of the whole water column at the same time of the day from May until October  
319 2013 and from February to May 2014. In May 2014 the diurnal pattern of the water density gradient  
320 was less pronounced than in May 2013.

### 321 **3.2 Gapfilling performance and annual budgeting of CO<sub>2</sub>, CH<sub>4</sub>, C and GWP**

322 The MDS<sub>CO<sub>2</sub>nofoot</sub> approach explained 74 % of the variance in NEE (see Table 2). Median NEE accounted  
323 for 1.9 g CO<sub>2</sub> m<sup>-2</sup> d<sup>-1</sup>. The annual budget of gapfilled NEE (MDS<sub>CO<sub>2</sub>nofoot</sub>) between 14 May 2013 and 14  
324 May 2014 was 524.5 ± 5.6 g CO<sub>2</sub> m<sup>-2</sup> (see Table 3), characterising the site as strong CO<sub>2</sub> source with  
325 moderate rates of R<sub>eco</sub> and GPP. We found a surprising CO<sub>2</sub> release strength during summer 2013,  
326 where already at the end of June daily R<sub>eco</sub> often exceeded GPP. The highest daily CO<sub>2</sub> emission and  
327 uptake rates of 24.8 g CO<sub>2</sub> m<sup>-2</sup> d<sup>-1</sup> and -27.9 g CO<sub>2</sub> m<sup>-2</sup> d<sup>-1</sup> were both revealed in the beginning of July  
328 2013 (see Fig. 2). July 2013 accounted for 23.2 % and 25.8 % of the annual R<sub>eco</sub> and GPP, respectively.  
329 In addition, net CO<sub>2</sub> release outside the growing season (definition of the growing season following  
330 Lund et al. 2010; until 19 November 2013 and starting 26 February 2014) was 203.7 g CO<sub>2</sub> m<sup>-2</sup> with a  
331 median of 2.2 g CO<sub>2</sub> m<sup>-2</sup> d<sup>-1</sup>.

332 The environmental variable giving the best NLR model for CH<sub>4</sub> was soil temperature in 10 cm depth  
333 (T<sub>s10</sub>):

$$334 F_{CH_4} = \exp(-7.224 + 0.313 \cdot T_{s10}) \quad (7)$$

335 The model described 79 % of the variance in CH<sub>4</sub> flux (see Table 2). Including additional environmental  
336 variables to the regression function did not increase the model performance significantly. Cumulative  
337 CH<sub>4</sub> emissions were 40.5 ± 0.2 g CH<sub>4</sub> m<sup>-2</sup> a<sup>-1</sup> (see Table 3). Median CH<sub>4</sub> emissions were 41.9 mg m<sup>-2</sup> d<sup>-1</sup>,  
338 peaked at the end of July 2013 with 0.6415 g CH<sub>4</sub> m<sup>-2</sup> d<sup>-1</sup> and were at the minimum in January 2014  
339 (see Fig. 2). The month with the highest proportion of annual CH<sub>4</sub> emissions was August 2013 (27.3 %).  
340 Non-growing season CH<sub>4</sub> fluxes only accounted for a small proportion within the annual budget, about  
341 0.8 g CH<sub>4</sub> m<sup>-2</sup>.

342 The site was an effective C and GHG source, accounting for 173.4 ± 1.7 g C m<sup>-2</sup> a<sup>-1</sup> and 1658.5 ± 11.2 g  
343 CO<sub>2</sub>-Eq. m<sup>-2</sup> a<sup>-1</sup> for the EC source area (see Fig. 4). The proportion of CO<sub>2</sub> in the C and GWP budget was  
344 82.5 % and 31.6 %, respectively. Components of the annual net C balance other than CO<sub>2</sub> and CH<sub>4</sub>  
345 fluxes, e.g. dissolved C, are not considered in this study. Our uncertainty estimates are within the range  
346 of similar studies (e.g. Shoemaker et al. 2015).

### 347 **3.3 Source area composition and spatial heterogeneity of CO<sub>2</sub> and CH<sub>4</sub>** 348 **exchange**

349 Footprint analysis revealed the peak contribution in an average distance of 18 m from the tower and  
350 mainly from the open water area of the shallow lake (see Fig. 5). Open water covered on average 62.5  
351 % of the EC source area. The two surface types showed different emission rates in terms of higher CH<sub>4</sub>  
352 fluxes and lower NEE rates with increasing Ω<sub>water</sub> (see Fig. 6). Within the NLR<sub>CO<sub>2</sub>foot</sub> approach both

353 surface types were denoted as sources of CO<sub>2</sub>, but with about 4-fold stronger rates of GPP, R<sub>eco</sub> and  
354 NEE for emergent vegetation compared to open water (see Fig. 7 and Table 3). The approach yielded  
355 a similar cumulative annual NEE for the whole EC source area including both surface types as the  
356 MDS<sub>CO2nofoot</sub> approach, but lower component fluxes (GPP and R<sub>eco</sub>). As for CO<sub>2</sub>, we implemented Ω<sub>i</sub> as  
357 weighting factors within the NLR model for CH<sub>4</sub> (NLR<sub>CH4foot</sub>) to get the surface type specific fluxes of CH<sub>4</sub>  
358 and fitted the parameters as follows:

$$359 \quad F_{CH_4} = \Omega_{veg} \cdot \exp(-10.076 + 0.415 \cdot T_{s10}) + \Omega_{water} \cdot \exp(-6.449 + 0.286 \cdot T_{s10}) \quad (8)$$

360 Open water accounted for more than 4-fold higher emissions than the vegetated areas (see Fig. 7 and  
361 Table 3). The NLR<sub>CH4foot</sub> approach revealed a similar annual CH<sub>4</sub> budget as the NLR<sub>CH4nofoot</sub> approach.

362 Annual budgets of CO<sub>2</sub> (844 g CO<sub>2</sub> m<sup>-2</sup> a<sup>-1</sup>) and CH<sub>4</sub> (22 g CH<sub>4</sub> m<sup>-2</sup> a<sup>-1</sup>) for the AOI differed strongly from  
363 the budgets for the EC source area due to the contrasting emission rates of open water and emergent  
364 vegetation (see Table 3) and different fractional coverages of the surface types within the AOI and the  
365 EC source area. This resulted in a higher C loss (246.5 g C m<sup>-2</sup> a<sup>-1</sup>) and a lower GWP (1452.9 g CO<sub>2</sub>-Eq.  
366 m<sup>-2</sup> a<sup>-1</sup>) for the AOI than for the EC source area. In the following we will primarily discuss the budgets  
367 of the EC source area and the surface types.

368

## 369 **4 Discussion**

### 370 **4.1 Diurnal variability of CH<sub>4</sub> emissions**

371 In terms of its daily cycle, CH<sub>4</sub> exchange between wetland ecosystems and the atmosphere is not  
372 generalisable, but rather dependent on the spatial characteristics of the wetland and thus, the impact  
373 of the individual CH<sub>4</sub> emission pathways (diffusion, ebullition, plant-mediated transport). Our  
374 measurements showed a diurnal cycle of CH<sub>4</sub> exchange from June to September 2013 and in March  
375 2014, with the strongest emissions during night, as reported for shallow lakes (e.g. Podgrasjek et al.  
376 2014) and wetland sites with a considerable fraction of open water (e.g. Godwin et al. 2013). In  
377 comparison, wetland CH<sub>4</sub> emissions were also reported to show daily maxima at day-time (e.g.  
378 Morrissey et al. 1993, Hendriks et al. 2010, Hatala Matthes et al. 2014), especially at sites with high  
379 abundance of vascular plants. No diurnal pattern (e.g. Rinne et al. 2007, Forbrich et al. 2011, Herbst et  
380 al. 2011) occurred especially at sites without large open water areas (Godwin et al. 2013).

381 We assume the process of convective mixing of the water column (e.g. Godwin et al. 2013, Poindexter  
382 and Variano 2013, Podgrajsek et al. 2014, Sahlée et al. 2014, Koebsch et al. 2015) to be crucial for the  
383 diurnal pattern of CH<sub>4</sub> emissions at our study site. This is indicated by the concurrent timing of  
384 convective mixing and daily peak CH<sub>4</sub> emissions and a generally high fractional source area coverage

385 of the open water, which shows higher rates of CH<sub>4</sub> release than emergent vegetation. Furthermore,  
386 closed chamber measurements likewise show night-time peak emissions on the shallow lake in  
387 summer 2013 (Hoffmann et al. 2015). During the day, CH<sub>4</sub> is trapped in the lower (anoxic) layers of the  
388 thermally stratified water column. Due to the heat release of the surface water to the atmosphere in  
389 the night the surface water cools down, initiating convective mixing of the water column down to the  
390 bottom. Diffusion is enhanced due to the buoyancy-induced turbulence, the associated increased gas  
391 transfer velocity at the air-water interface (Eugster et al. 2003, MacIntyre et al. 2010, Podgrajsek et al.  
392 2014) as well as the transport of CH<sub>4</sub> enriched bottom water to the surface (Godwin et al. 2013,  
393 Podgrajsek et al. 2014). In addition, ebullition can be triggered by turbulence due to convective mixing  
394 (Podgrajsek et al. 2014, Read et al. 2012). Apart from convective mixing, highest sediment and soil  
395 temperature in the night until early morning might play an important role for the peak emissions of  
396 CH<sub>4</sub> due to increased microbial activity. Furthermore, diurnal variability in CH<sub>4</sub> oxidation could  
397 contribute to the daily pattern of CH<sub>4</sub> release. Oxygen is supplied to the water, sediment and soil during  
398 the day in consequence of photosynthesis and increases CH<sub>4</sub> oxidation. However, convective mixing of  
399 the water column during the night might supply oxygen to deeper water depths potentially increasing  
400 CH<sub>4</sub> oxidation. We assume plant-mediated transport to be characterised by a reverse diurnal cycle with  
401 peak emissions during day-time, as the release of methane is dependent on the stomatal conductance  
402 of the plants (e.g. Morrissey et al. 1993). This pathway is limited to plants with aerenchymatic tissue  
403 like *Typha latifolia*, which dominates the eulittoral zone at our study site. CH<sub>4</sub> is transported from the  
404 soil to the atmosphere, bypassing potential oxidation zones above the rhizosphere (chimney effect).  
405 Unusually for wetland plants (Torn and Chapin 1993), complete stomatal closure during night was  
406 observed for *Typha latifolia* (Chanton et al. 1993). However, this temporal constraint seems to be  
407 superimposed by more efficient CH<sub>4</sub> pathways during the night and early morning. Apart from CH<sub>4</sub>,  
408 thermally induced convection potentially contributes also to the diurnal fluctuation of the CO<sub>2</sub> flux at  
409 our study site. According to Eugster et al. (2003) penetrative convection might be the dominant  
410 mechanism yielding CO<sub>2</sub> fluxes during periods of low wind speed, especially in case of a stratification  
411 of CO<sub>2</sub> concentrations in the water body. Ebullition triggered by convective mixing might be less  
412 important for CO<sub>2</sub> than for CH<sub>4</sub>, as concentrations of CO<sub>2</sub> are most often low in gas bubbles (e.g. Casper  
413 et al. 2000, Poissant et al. 2007, Repo et al. 2007, Sepulveda-Jauregui et al. 2015, Spawn et al. 2015).  
414 Further investigations should focus on the controls of the diurnal patterns in CO<sub>2</sub> and CH<sub>4</sub> exchange  
415 based on additional measurements, e.g. gas concentrations in the water, methane oxidation or plant-  
416 mediated transport.

## 417 4.2 Annual CH<sub>4</sub> emissions

418 The CH<sub>4</sub> emissions of our studied ecosystem were within the range of other temperate fen sites  
419 rewetted for several years (up to 63 g CH<sub>4</sub> m<sup>-2</sup> a<sup>-1</sup>; e.g. Hendriks et al. 2007, Wilson et al. 2008, Günther  
420 et al. 2013, Schrier-Uijl et al. 2014). This rate is remarkably higher than the emission factor of 28.8 g  
421 CH<sub>4</sub> m<sup>-2</sup> a<sup>-1</sup> that was assigned to rewetted temperate rich organic soils, which is in turn more than twice  
422 the rate of the nutrient-poor complement (IPCC 2014). In contrast, newly rewetted fens emit its  
423 multiple. In the first year after flooding, Hahn et al. (2015) observed at a fen site in NE Germany an  
424 average net release of 260 g CH<sub>4</sub> m<sup>-2</sup> a<sup>-1</sup>, which is 186 times higher than before flooding,. Two years  
425 later the CH<sub>4</sub> emissions were considerably lower (40 g CH<sub>4</sub> m<sup>-2</sup> within the growing season; Koebisch et  
426 al. 2015). However, natural (e.g. Bubier et al. 1993, Nilsson et al. 2001) and degraded fens (Hatala et  
427 al. 2012, Schrier-Uijl et al. 2014, see also IPCC 2014) release most often less CH<sub>4</sub> than the majority of  
428 rewetted fens, with some exceptions (e.g. Huttunen et al. 2003).

429 The two main surface types open water and emergent vegetation differed substantially in their CH<sub>4</sub>  
430 exchange rates. Open water contributed overproportionally to the measured ecosystem fluxes and  
431 showed remarkably higher CH<sub>4</sub> release rates (52.6 g CH<sub>4</sub> m<sup>-2</sup> a<sup>-1</sup>) than the emergent vegetation stands  
432 (13.2 g CH<sub>4</sub> m<sup>-2</sup> a<sup>-1</sup>). However, closed-chamber measurements at the shallow lake show an even higher  
433 long-term average annual CH<sub>4</sub> release rate (206 g CH<sub>4</sub> m<sup>-2</sup> a<sup>-1</sup>) since rewetting with large interannual  
434 variability and occasionally extreme high release rates (up to 400 g CH<sub>4</sub> m<sup>-2</sup> a<sup>-1</sup>; Casares et al., in prep.).

435 We assume the permanent high inundation and high productivity due to eutrophic conditions, feeding  
436 the organic mud deposited at the bottom of the open water body (which is typical for shallow lakes in  
437 rewetted fens), to be of particular importance for high CH<sub>4</sub> emissions as substrate for decomposition.  
438 The mud initially evolved as a mixture of sand and easily decomposable labile plant litter from reed  
439 canary grass, which died-off after flooding and produced a large C pool for CH<sub>4</sub> production (Hahn-Schöfl  
440 et al 2011). During an incubation experiment with substrate from our study site Hahn-Schöfl et al.  
441 (2011) observed that the new sediment layer has very high specific rates of anaerobic CH<sub>4</sub> (and CO<sub>2</sub>)  
442 production. In addition, Zak et al. (2015) emphasised the impact of litter quality and reported a very  
443 high CH<sub>4</sub> production potential for litter of *Ceratophyllum demersum*, which dominates the biomass in  
444 the open water at our study site. Due to the eutrophic character of the lake and associated high  
445 productivity within the open water body and in the eulittoral zone, high amounts of fresh labile organic  
446 matter continuously replenish the mud layer and thus the C pool. Especially in case of strong winds we  
447 further assume a lateral input of allochthonous organic matter into the NE "bay" of the shallow lake,  
448 which is the area with the peak contribution of our EC derived fluxes, and thus an additional refill of  
449 the C pool. The importance of fresh labile organic matter provided by the die-back of the former

450 vegetation as driving force for high CH<sub>4</sub> emissions was also discussed in Hahn et al. (2015). They  
451 measured the highest CH<sub>4</sub> emissions in sedge stands suffering from strongest die-back.

452 For comparison annual budgets of CH<sub>4</sub> and CO<sub>2</sub> for other nutrient-rich lentic freshwater ecosystems in  
453 terms of pristine, anthropogenically influenced and transient ecosystems are listed in Table 4. Studies  
454 on nutrient-rich lakes generally revealed lower CH<sub>4</sub> release for open water. In contrast, beaver ponds  
455 were partially reported to emit comparable rates of CH<sub>4</sub>. Similarly to our study site beaver ponds are  
456 at least in the beginning disbalanced ecosystems due to a rapidly increased water level with associated  
457 suffering and finally the die-back of former vegetation, which is not adapted to higher water levels. A  
458 large C pool for CH<sub>4</sub> production develops. However, even for a beaver pond existing more than 30 years  
459 CH<sub>4</sub> emissions still accounted for 40 g CH<sub>4</sub> m<sup>-2</sup> a<sup>-1</sup> (Yavitt et al. 1992).

460 The lower CH<sub>4</sub> emissions of the surface type emergent vegetation might be the result of increased CH<sub>4</sub>  
461 oxidation in the soil, as plants with aerenchymatic tissue release oxygen into the rhizosphere, in  
462 reverse to the emission of CH<sub>4</sub> into the atmosphere (Bhullar et al. 2013). Minke et al. (2015) highlight  
463 the difference in net CH<sub>4</sub> release for typical helophyte stands with moderate emissions for *Typha*  
464 dominated sites. Besides the effect of the gas transport within plants, lower water and sediment  
465 temperatures due to shading by the emergent vegetation might yield lower CH<sub>4</sub> production than for  
466 open water. Furthermore, the soil of emergent vegetation stands is generally only temporarily and  
467 partly inundated and the water table decreased additionally during the unusual warm and dry summer  
468 2013, probably resulting in a lower rate of anaerobic decomposition to CH<sub>4</sub> and a higher rate of CH<sub>4</sub>  
469 oxidation in the aerated top soil. This in turn might be a reason, that in comparison to other sites  
470 dominated by *Typha* (rewetted wetlands, lake shores and freshwater marshes; see Table 4) the  
471 emergent vegetation at our site is at the lower limit of reported CH<sub>4</sub> release rates and best comparable  
472 to closed chamber measurements of *Typha latifolia* microsites at another rewetted fen site in NE  
473 Germany (Günther et al. 2015).

### 474 **4.3 Annual net CO<sub>2</sub> release**

475 We observed high annual net release of CO<sub>2</sub> during the observation period, which is rather uncommon  
476 for fens several years after rewetting (e.g. Hendriks et al. 2007, Schrier-Uijl et al. 2014, Knox et al.  
477 2015). Surprisingly, the net CO<sub>2</sub> budget was higher or similar to those of some drained and degraded  
478 peatlands (e.g. Hatala et al. 2012, Schrier-Uijl et al. 2014, but IPCC 2014). Both surface types acted as  
479 net sources, with emergent vegetation (750 g CO<sub>2</sub> m<sup>-2</sup> a<sup>-1</sup>) showing a distinctively higher net budget  
480 (158 g CO<sub>2</sub> m<sup>-2</sup> a<sup>-1</sup>) as well as GPP and R<sub>eco</sub> rates than open water. Only few NEE rates are published for  
481 the open water body of eutrophic shallow lakes. Ducharme-Riel et al. (2015) report 224 g CO<sub>2</sub> m<sup>-2</sup> a<sup>-1</sup>  
482 as annual NEE of a eutrophic lake in Canada (see Table 4). According to Kortelainen et al. (2006) Finnish

483 lakes, which are mainly small and shallow, continuously emit CO<sub>2</sub> during the ice-free period, positively  
484 correlated with their trophic state.

485 Our study revealed a high annual net CO<sub>2</sub> release for emergent vegetation, which is in the wide range  
486 of NEE rates for *Typha* sites reported in other studies, including both net CO<sub>2</sub> sources and sinks (see  
487 Table 5). GPP and R<sub>eco</sub> are generally high (especially at rewetted fen sites; both component fluxes most  
488 often > 3000 g CO<sub>2</sub> m<sup>-2</sup> a<sup>-1</sup>), characterising *Typha* stands as high turnover sites, usually resulting in net  
489 CO<sub>2</sub> uptake. In contrast, R<sub>eco</sub> and GPP rates at our study site are in the lower part of the reported range.  
490 We assume the continuously high R<sub>eco</sub> rates during winter 2013/2014, contributing to the high annual  
491 net CO<sub>2</sub> emissions, to be the result of mild and dry meteorological conditions. In summer 2013, R<sub>eco</sub>  
492 exceeded GPP already in late June, indicating a significant contribution of heterotrophic respiration to  
493 the CO<sub>2</sub> production. Unusual warm and dry conditions and associated water table lowering during  
494 summer 2013 might have triggered a shift from anaerobic to aerobic decomposition due to the  
495 exposure of formerly only shallowly inundated soil and organic mud, primarily in the emergent  
496 vegetation stands. We could not observe a considerable decrease of the spatial extent of the open  
497 water body as emergent vegetation mainly covers the shallower edges of the water body. The effect  
498 of water table lowering at *Typha* sites due to dry conditions is also shown by Günther et al. (2015) and  
499 Chu et al. (2015): relative increase of R<sub>eco</sub> rates, resulting in net CO<sub>2</sub> release. This might be of special  
500 interest in terms of climate change, as a temperature increase and significantly less precipitation in  
501 summer are expected for NE Germany and meteorological conditions are more frequently  
502 characterised as “unusually” warm and dry. In addition, a considerable increase of microbial activity  
503 and thus, generally increased decomposition due to high temperatures might be of importance.  
504 Besides CH<sub>4</sub>, Hahn-Schöfl et al. (2011) showed that the new sediment layer at the bottom of inundated  
505 areas exhibits very high rates of anaerobic CO<sub>2</sub> production. Allochthonous organic matter import into  
506 the NE bay due to lateral transport, as discussed for CH<sub>4</sub>, might have further enhanced decomposition  
507 (e.g. Chu et al. 2015). Longer data gaps in summer 2013 (see Fig. A1) increase the uncertainty of our  
508 annual CO<sub>2</sub> budget. However, the observed shift to net CO<sub>2</sub> release starting in late June 2013 as well  
509 as its continuation later on are substantially based on measurements.

#### 510 **4.4 Global warming potential and the impact of spatial heterogeneity**

511 The lake ecosystem is characterised by a strong climate impact 9 years after rewetting, mainly driven  
512 by high CH<sub>4</sub> emissions. Based on our results the site can hardly be classified into any rewetting phase  
513 of the concept discussed by Augustin and Joosten (2007). Our results imply a delayed shift of the  
514 ecosystem towards a C sink with reduced climate impact, which might be the result of the exceptional  
515 characteristics represented by eutrophic conditions and lateral transport of organic matter within the  
516 open water body. The trophic status of water and sediment is an important factor regulating GHG



517 emissions, as shown by Schrier-Uijl et al. (2011) for lakes and drainage ditches in wetlands. However,  
518 the unusual meteorological conditions during our study period might have caused a differing (lower or  
519 higher) GWP compared to previous years. CH<sub>4</sub> emissions might have been lower at the expense of high  
520 net CO<sub>2</sub> release, whereas under usual meteorological conditions e.g. CO<sub>2</sub> uptake could probably  
521 compensate the CH<sub>4</sub> emissions. Inundation is generally associated with high CH<sub>4</sub> emission. Thus, during  
522 rewetting the water table is generally recommended to be held at or just below the soil surface to  
523 prevent inundation and the formation of organic mud (Couwenberg et al. 2011, Joosten et al. 2012,  
524 Zak et al. 2015).

525 In contrast to CH<sub>4</sub>, the influence of water level on net CO<sub>2</sub> release is not nearly consistent in the few  
526 existing studies of rewetted peatlands. In comparison to our site Knox et al. (2015) reported high net  
527 CO<sub>2</sub> uptake to substantially compensate high CH<sub>4</sub> emissions for a site with mean water levels above  
528 the soil surface after several years of rewetting (see Table 5). Similarly, Schrier-Uijl et al. (2014)  
529 reported high CO<sub>2</sub> uptake rates for a Dutch fen site 7 years after rewetting and even C uptake and a  
530 GHG sink function after 10 years with water levels below or at the soil surface. Herbst et al. (2011)  
531 present a snapshot of the GHG emissions of a Danish site after 5 years of rewetting with permanently  
532 and seasonally wet areas, whereby high CO<sub>2</sub> uptake and moderate CH<sub>4</sub> emissions lead to substantial  
533 GHG savings. In contrast, weak CO<sub>2</sub> uptake and decreasing, but still high CH<sub>4</sub> emissions were reported  
534 for another fen site in NE Germany with mean water levels above the soil surface (Koebsch et al. 2013,  
535 2015 and Hahn et al. 2015), resulting in a decreasing climate impact after 3 years of rewetting.  
536 Interestingly, changes of NEE due to flooding were negligible, although GPP and R<sub>eco</sub> rates decreased  
537 considerable due to the flooding (Koebsch et al. 2013). In comparison to the decreasing CH<sub>4</sub> emissions  
538 at this site, Waddington and Day (2007) report enhancing CH<sub>4</sub> release for a Canadian peatland in the  
539 first 3 years after rewetting. A third rewetted fen site in NE Germany with water levels close to the soil  
540 surface was reported as weak GHG source 14-15 years after rewetting (Günther et al. 2015).

541 We calculated the “true” fluxes of CO<sub>2</sub> and CH<sub>4</sub> for the AOI by weighting the NLR functions for the two  
542 surface types with their fractional coverage inside the AOI. The inferred C budget and global warming  
543 potential differs considerably from that of the EC source area, highlighting the strikingly different  
544 emission rates of open water versus emergent vegetation. Thus, footprint analysis providing the  
545 fractional coverage of the main surface types is imperative for the interpretation of ecosystem flux  
546 measurements as provided by the EC technique at such a spatially heterogeneous site. In addition, for  
547 an interannual comparison of EC derived budgets for such sites it is necessary to define a fixed AOI, as  
548 the cumulative footprint climatology (representing the EC source area) changes interannually. Inter-  
549 site comparisons (e.g. with other shallow lakes evolved during fen rewetting) are challenging with  
550 regard to the site-specific spatial heterogeneity and their interannual variability, if short-term studies

551 like the present one are involved. Comparisons might be misleading in case the fractional coverages of  
552 the main surface types are not considered. Furthermore, as shown by Wilson et al. (2007, 2008) and  
553 Minke et al. (2015) vegetation composition has a remarkable effect on GHG emissions of rewetted  
554 peatlands and should be considered within inter-site comparisons.

555

## 556 **5 Conclusions**

557 This study contributes to the understanding of eutrophic shallow lakes as a challenging ecosystem  
558 often evolving during fen rewetting. Within the study period the ecosystem was a strong source of CH<sub>4</sub>  
559 and CO<sub>2</sub>. Both open water and emergent vegetation, particularly including the eulittoral zone, were  
560 net emitters of CH<sub>4</sub> and CO<sub>2</sub>, but with strikingly different release rates. This illustrates the importance  
561 of footprint analysis for the interpretation of the EC measurements on a rewetted site with distinct  
562 spatial heterogeneity. The strong climate impact of the lake is dominated by considerable CH<sub>4</sub> release,  
563 particularly from the open water section. A comparison with existing chamber measurements at the  
564 open water body for the same time period will be helpful for the evaluation of our measurements and  
565 estimation of the surface type fluxes. The site is gradually changing, with helophytes (especially *Typha*  
566 *latifolia*) progressively entering the open water body in the course of terrestrialisation. Peat formation  
567 and C uptake might be initiated once the shallow lake is inhabited by peat-forming vegetation and  
568 replenished by organic sediments. Therefore, long-term measurements are necessary to evaluate the  
569 impact of future ecosystem development on GHG emissions. Interannual comparisons are also  
570 necessary to verify what the results of this study imply: that the intended effects of rewetting in terms  
571 of CO<sub>2</sub> emission reduction and C sink recovery are not yet achieved at this site. In this context, the  
572 effect of unusual meteorological conditions needs further investigation. More general statements for  
573 the climate impact of rewetted fens can only be provided by inclusion of additional sites varying e.g.  
574 in groundwater table and plant composition. We assume that shallow lakes represent a special case  
575 with regard to the GHG dynamics and climate impact, with exceptionally high CH<sub>4</sub> release and  
576 occasionally high net CO<sub>2</sub> emissions. Our study shows that permanent (high) inundation in combination  
577 with nutrient-rich conditions involves the risk of long-term high CH<sub>4</sub> emissions. They counteract the  
578 actually intended lowering of the climate impact of drained and degraded fens and can result in an  
579 even stronger climate impact than degraded fens, as also shown in previous studies. We strongly  
580 recommend to consider this risk in future rewetting projects and support the call of Lamers et al. (2015)  
581 for the need of well-conceived restoration management instead of the trial-and-error approach,  
582 whereon restoration of wetland ecosystem services was based for a long time.

583

584 **Appendix A**

585 Measurement data coverage of CO<sub>2</sub> and CH<sub>4</sub> fluxes within the study period is shown in Fig. A1.

586

587 **Data availability**

588 Processed eddy covariance flux and meteorological data of this study site (site code DE-Zrk) are  
589 available at <http://www.europe-fluxdata.eu>.

590

591 **Acknowledgements**

592 This work was supported by the Helmholtz Association of German Research Centres through a  
593 Helmholtz Young Investigators Group to T.S. (grant VH-NG-821) and is a contribution to the Helmholtz  
594 Climate Initiative REKLIM (Regional Climate Change). Infrastructure funding through the Terrestrial  
595 Environmental Observatories Network (TERENO) is also acknowledged. We thank M. Hoffmann (ZALF,  
596 Müncheberg, Germany) and C. Hohmann (GFZ Potsdam, Germany) for providing meteorological data.  
597

598 **References**

- 599 Aubinet, M., Feigenwinter, C., Heinesch, B., Laffineur, Q., Papale, D., Reichstein, M., Rinne, J. and Van  
600 Gorsel, E.: Nighttime flux correction, in: *Eddy Covariance: A practical guide to measurement and*  
601 *data analysis*, Springer Atmospheric Sciences, edited by Aubinet, M., Vesala, T. and Papale, D.,  
602 Springer Netherlands, Dordrecht, doi:10.1007/978-94-007-2351-1, 133-158, 2012.
- 603 Augustin, J. and Joosten, H.: Peatland rewetting and the greenhouse effect, *International Mire*  
604 *Conservation Group Newsletter*, 3, 29-30, 2007.
- 605 Barcza, Z., Kern, A., Haszpra, L. and Kljun, N.: Spatial representativeness of tall tower eddy covariance  
606 measurements using remote sensing and footprint analysis, *Agr. Forest Meteorol.*, 149, 795-807,  
607 doi: 10.1016/j.agrformet.2008.10.021, 2009.
- 608 Bastviken, D., Cole, J., Pace, M. and Tranvik, L.: Methane emissions from lakes: Dependence of lake  
609 characteristics, two regional assessments, and a global estimate, *Global Biogeochem. Cy.*, 18,  
610 GB4009, doi: 10.1029/2004GB002238, 2004.
- 611 Beetz, S., Liebersbach, H., Glatzel, S., Jurasinski, G., Buczko, U. and Höper, H.: Effects of land use  
612 intensity on the full greenhouse gas balance in an Atlantic peat bog, *Biogeosciences*, 10, 1067-  
613 1082, doi:10.5194/bg-10-1067-2013, 2013.
- 614 Berg, E., Jeschke, L. and Lenschow, U.: Das Moorschutzkonzept Mecklenburg-Vorpommern, *Telma*, 30,  
615 173-220, 2000.
- 616 Béziat, P., Ceschia, E. and Dedieu, G.: Carbon balance of a three crop succession over two cropland  
617 sites in South West France, *Agr. Forest Meteorol.*, 149, 1628-1645,  
618 doi:10.1016/j.agrformet.2009.05.004, 2009.
- 619 Bhullar, G. S., Edwards, P. J. and Olde Venterink, H.: Variation in the plant-mediated methane transport  
620 and its importance for methane emission from intact wetland peat mesocosms, *J. Plant Ecol.*, 6,  
621 298-304, doi: 10.1093/jpe/rts045, 2013.
- 622 Bignell, N.: The effect of dissolved air on the density of water, *Metrologia*, 19, 57-59, 1983.
- 623 Bonneville, M.-C., Strachan, I. B., Humphreys, E. R. and Roulet, N. T.: Net ecosystem CO<sub>2</sub> exchange in a  
624 temperate cattail marsh in relation to biophysical properties, *Agr. Forest Meteorol.*, 148, 69-81,  
625 doi:10.1016/j.agrformet.2007.09.004, 2008.
- 626 Bubier, J. L., Moore, T. R. and Roulet, N. T.: Methane emissions from wetlands in the Midboreal Region  
627 of Northern Ontario, Canada, *Ecology*, 74, 2240-2254, 1993.

628 Casper, P., Maberly, S. C., Hall, G. H. and Finlay, B. J.: Fluxes of methane and carbon dioxide from a  
629 small productive lake to the atmosphere, *Biogeochemistry*, 49, 1-19, doi:  
630 10.1023/A:1006269900174, 2000.

631 Chanton, J. P., Whiting, G. J., Happell, J. D. and Gerard, G.: Contrasting rates and diurnal patterns of  
632 methane emission from different types of vegetation, *Aquat. Bot.*, 46, 111-128, 1993.

633 Chen, B., Coops, N. C., Fu, D., Margolis, H. A., Amiro, B. D., Barr, A. G., Black, T. A., Arain, M. A., Bourque,  
634 C. P.-A., Flanagan, L. B., Lafleur, P. M., McCaughey, J. H. and Wofsy, S. C.: Assessing eddy-  
635 covariance flux tower location bias across the Fluxnet-Canada Research Network based on remote  
636 sensing and footprint modelling, *Agr. Forest Meteorol.*, 151, 87–100,  
637 doi:10.1016/j.agrformet.2010.09.005, 2011.

638 Chu, H., Gottgens, J. F., Chen, J., Sun, G., Desai, A. R., Ouyang, Z., Shao, C. and Czajkowski, K.: Climatic  
639 variability, hydrologic anomaly, and methane emission can turn productive freshwater marshes  
640 into net carbon sources, *Glob. Change Biol.*, 21, 1165-1181, doi: 10.1111/gcb.12760, 2015.

641 Couwenberg, J., Thiele, A., Tanneberger, F., Augustin, J., Bärtsch, S., Dubovik, D., Liashchynskaya, N.,  
642 Michaelis, D., Minke, M., Skuratovich, A. and Joosten, H.: Assessing greenhouse gas emissions  
643 from peatlands using vegetation as a proxy, *Hydrobiologia*, 674, 67-89, doi:10.1007/s10750-011-  
644 0729-x, 2011.

645 Dengel, S., Levy, P. E., Grace, J., Jones, S. K. and Skiba, U. M.: Methane emissions from sheep pasture,  
646 measured with an open-path eddy covariance system, *Glob. Change Biol.*, 17, 3524-3533, doi:  
647 10.1111/j.1365-2486.2011.02466.x, 2011.

648 Ducharme-Riel, V., Vachon, D., del Giorgio, P. A. and Prairie, Y. T.: The relative contribution of winter  
649 under-ice and summer hypolimnetic CO<sub>2</sub> accumulation to the annual CO<sub>2</sub> emissions from  
650 northern lakes, *Ecosystems*, 18, 547-559, doi:10.1007/s10021-015-9846-0, 2015.

651 Eugster, W., Kling, G., Jonas, T., McFadden, J. P., Wüest, A., MacIntyre, S. and Chapin III, F. S.: CO<sub>2</sub>  
652 exchange between air and water in an Arctic Alaskan and midlatitude Swiss lake: importance of  
653 convective mixing, *J. Geophys. Res.*, 108, 4362, doi: 10.1029/2002JD002653, 2003.

654 Falge, E., Baldocchi, D., Olson, R. J., Anthoni, P., Aubinet, M., Bernhofer, C., Burba, G., Ceulemans, R.,  
655 Clement, R., Dolman, H., Granier, A., Gross, P., Grünwald, T., Hollinger, D., Jensen, N.-O., Katul, G.,  
656 Keronen, P., Kowalski, A., Ta Lai, C., Law, B. E., Meyers, T., Moncrieff, J., Moors, E., Munger, J. W.,  
657 Pilegaard, K., Rannik, Ü., Rebmann, C., Suyker, A., Tenhunen, J., Tu, K., Verma, S., Vesala, T.,  
658 Wilson, K. and Wofsy, S. C.: Gap filling strategies for defensible annual sums of net ecosystem  
659 exchange, *Agr. Forest Meteorol.*, 107, 43–69, doi:10.1016/S0168-1923(00)00225-2, 2001.

660 Fan, S.-M., Wofsy, S. C., Bakwin, P. S., Jacob, D. J. and Fitzjarrald, D. R.: Atmosphere-biosphere  
661 exchange of CO<sub>2</sub> and O<sub>3</sub> in the Central Amazon Forest, *J. Geophys. Res.*, 95, 16851-16864, 1990.

662 Finkelstein, P. L. and Sims, P. F.: Sampling error in eddy correlation flux measurements, *J. Geophys.*  
663 *Res.-Atmos.*, 106, 3503-3509, doi:10.1029/2000JD900731, 2001.

664 Finnigan, J. J., Clement, R., Mahli, Y., Leuning, R. and Cleugh, H. A.: A re-evaluation of long-term flux  
665 measurement techniques. Part I: Averaging and coordinate rotation, *Bound.-Lay. Meteorol.*, 107,  
666 1-48, doi:10.1023/A:1021554900225, 2003.

667 Foken, T.: *Micrometeorology*. Springer, Berlin, 308 pp, doi:10.1007/978-3-540-74666-9, 2008.

668 Forbrich, I., Kutzbach, L., Wille, C., Becker, T., Wu, J. and Wilmking, M.: Cross-evaluation of  
669 measurements of peatland methane emissions on microform and ecosystem scales using high-  
670 resolution landcover classification and source weight modelling, *Agr. Forest Meteorol.*, 151, 864-  
671 874, doi:10.1016/j.agrformet.2011.02.006, 2011.

672 Fratini, F., Ibrom, A., Arriga, N., Burba, G. and Papale, D.: Relative humidity effects of water vapour  
673 fluxes measured with closed-path eddy-covariance systems with short sampling lines, *Agr. Forest*  
674 *Meteorol.*, 165, 53-63, 2012.

675 Frolking, S., Talbot, J., Jones, M. C., Treat, C. C., Kauffman, J. B., Tuittila, E.-S. and Roulet, N. T.: Peatlands  
676 in the earth's 21st century climate system, *Environ. Rev.*, 19, 371-396, doi:10.1139/a11-014, 2011.

677 Göckede, M., Rebmann, C. and Foken, T.: A combination of quality assessment tools for eddy  
678 covariance measurements with footprint modelling for the characterisation of complex sites, *Agr.*  
679 *Forest Meteorol.*, 127, 175-188, doi:10.1016/j.agrformet.2004.07.012, 2004.

680 Godwin, C. M., McNamara, P. J. and Markfort, C. D.: Evening methane emission pulses from a boreal  
681 wetland correspond to convective mixing in hollows, *J. Geophys. Res.-Biogeo.*, 118, 994-1005, doi:  
682 10.1002/jgrg.20082, 2013.

683 Günther, A. B., Huth, V., Jurasinski, G. and Glatzel, S.: Scale-dependent temporal variation in  
684 determining the methane balance of a temperate fen, *Greenhouse Gas Measurement and*  
685 *Management*, 4, 41-48, doi: 10.1080/20430779.2013.850395, 2013.

686 Günther, A. B., Huth, V., Jurasinski, G. and Glatzel, S.: The effect of biomass harvesting on greenhouse  
687 gas emissions from a rewetted temperate fen, *GCB Bioenergy*, 7, 1092-1106, doi:  
688 10.1111/gcbb.12214, 2015.

689 Hahn, J., Köhler, S., Glatzel, S. and Jurasinski, G.: Methane exchange in a coastal fen in the first year  
690 after flooding – A systems shift, *PLoS ONE*, 10, e0140657, doi:10.1371/journal.pone.0140657,  
691 2015.

692 Hahn-Schöfl, M., Zak, D., Minke, M., Gelbrecht, J., Augustin, J. and Freibauer, A.: Organic sediment  
693 formed during inundation of a degraded fen grassland emits large fluxes of CH<sub>4</sub> and CO<sub>2</sub>,  
694 *Biogeosciences*, 8, 1539-1550, doi:10.5194/bg-8-1539-2011, 2011.

695 Hatala, J., Detto, M., Sonnentag, O., Deverel, S. J., Verfaillie, J. and Baldocchi, D. D.: Greenhouse gas  
696 (CO<sub>2</sub>, CH<sub>4</sub>, H<sub>2</sub>O) fluxes from drained and flooded agricultural peatlands in the Sacramento-San  
697 Joaquin Delta, *Agr. Ecosyst. Environ.*, 150, 1-18, doi:10.1016/j.agee.2012.01.009, 2012.

698 Hatala Matthes, J., Sturtevant, C., Verfaillie, J., Knox, S. and Baldocchi, D.: Parsing the variability in CH<sub>4</sub>  
699 flux at a spatially heterogeneous wetland: Integrating multiple eddy covariance towers with high-  
700 resolution flux footprint analysis, *J. Geophys. Res.-Biogeo.*, 119, 1322-1339,  
701 doi:10.1002/2014JG002642 2014.

702 Hendriks, D. M. D., van Huissteden, J., Dolman, A. J. and van der Molen, M. K.: The full greenhouse gas  
703 balance of an abandoned peat meadow, *Biogeosciences*, 4, 411-424, doi:10.5194/bg-4-411-2007,  
704 2007.

705 Hendriks, D. M. D., van Huissteden, J. and Dolman, A. J.: Multi-technique assessment of spatial and  
706 temporal variability of methane fluxes in a peat meadow, *Agr. Forest Meteorol.*, 150, 757-774,  
707 doi:10.1016/j.agrformet.2009.06.017, 2010.

708 Herbst, M., Friborg, T., Ringgaard, R. and Soegaard, H.: Interpreting the variations in atmospheric  
709 methane fluxes observed above a restored wetland, *Agr. Forest Meteorol.*, 151, 841-853,  
710 doi:10.1016/j.agrformet.2011.02.002, 2011.

711 Hoffmann, M., Schulz-Hanke, M., Garcia Alba, J., Jurisch, N., Hagemann, U., Sachs, T., Sommer, M. and  
712 Augustin, J.: Technical Note: A simple calculation algorithm to separate high-resolution CH<sub>4</sub> flux  
713 measurements into ebullition and diffusion-derived components, *Biogeosciences Discussions*, 12,  
714 12923-12945, doi:10.5194/bgd-12-12923-2015, 2015.

715 Holden, J., Chapman, P. J. and Labadz, J. C.: Artificial drainage of peatlands: hydrological and  
716 hydrochemical process and wetland restoration, *Prog. Phys. Geog.*, 28, 95-123,  
717 doi:10.1191/0309133304pp403ra, 2004.

718 Hommeltenberg, J., Mauder, M., Drösler, M., Heidbach, K., Werle, P. and Schmid, H. P.: Ecosystem  
719 scale methane fluxes in a natural temperate bog-pineforest in southern Germany, *Agr. Forest  
720 Meteorol.*, 198-199, 273-284, doi:10.1016/j.agrformet.2014.08.017, 2014.

721 Höper, H., Augustin, J., Cagampan, J. P., Drösler, M., Lundin, L., Moors, E., Vasander, H., Waddington,  
722 J. M., and Wilson, D.: Restoration of peatlands and greenhouse gas balances, in: *Peatlands and  
723 climate change*, edited by Strack, M., International Peat Society, Jyväskylä, 182-210, 2008.

724 Horst, T. W. and Lenschow, D. H.: Attenuation of scalar fluxes measured with spatially-displaced  
725 sensors, *Bound.-Lay. Meteorol.*, 130, 275-300, doi:10.1007/s10546-008-9348-0, 2009.

726 Huttunen, J. T., Nykänen, H., Turunen, J. and Martikainen, P. J.: Methane emissions from natural  
727 peatlands in the northern boreal zone in Finland, Fennoscandia, *Atmos. Environ.*, 37, 147-151,  
728 doi:10.1016/S1352-2310(02)00771-9, 2003.

729 IPCC: Climate Change 2013: The physical science basis. Contribution of Working Group I to the Fifth  
730 Assessment Report of the Intergovernmental Panel on Climate Change, edited by Stocker, T. F.,  
731 Qin, D., Plattner, G.-K., Tignor, M. M. B., Allen, S. K., Boschung, J., Nauels, A., Xia, Y., Bex, V. and  
732 Midgley, P. M., Cambridge University Press, Cambridge, New York, 1535 pp,  
733 doi:10.1017/CBO9781107415324, 2013.

734 IPCC: 2013 Supplement to the 2006 IPCC Guidelines for National Greenhouse Gas Inventories:  
735 Wetlands, edited by Hiraishi, T., Krug, T., Tanabe, K., Srivastava, N., Baasansuren, J., Fukuda, M.  
736 and Troxler, T.G., IPCC, Switzerland, 354 pp, 2014.

737 Itzerott, S.: TERENO (Northeast), Climate station Karlshof, Germany. Deutsches  
738 GeoForschungsZentrum GFZ. <http://dx.doi.org/10.5880/TERENO.265>, 2015.

739 Joosten, H.: The global peatland CO<sub>2</sub> picture – Peatland status and drainage related emissions in all  
740 countries of the world, *Wetlands International*, Ede, 36 pp, 2010.

741 Joosten, H., Tapio-Biström, M.-L. and Tol, S. (Eds.): Peatlands – guidance for climate change mitigation  
742 through conservation, rehabilitation and sustainable use, 2nd edition, Food and Agriculture  
743 Organization of the United Nations and Wetlands International, 100 pp, 2012.

744 Juutinen, S., Alm, J., Larmola, T., Huttunen, J. T., Morero, M., Martikainen, P. J. and Silvola, J.: Major  
745 implication of the littoral zone for methane release from boreal lakes, *Global Biogeochem. Cy.*,  
746 17, 1117, doi:10.1029/2003GB002105, 2003.

747 Kankaala, P., Ojala, A. and Käki, T.: Temporal and spatial variation in methane emissions from a flodded  
748 transgression shore of a boreal lake, *Biogeochemistry*, 68, 297-311, doi:  
749 10.1023/B:BIOG.0000031030.77498.1f, 2004.

750 Knox, S. H., Sturtevant, C., Hatala Matthes, J., Koteen, L., Verfaillie, J. and Baldocchi, D.: Agricultural  
751 peatland restoration: effects of land-use change on greenhouse gas (CO<sub>2</sub> and CH<sub>4</sub>) fluxes in the  
752 Sacramento-San Joaquin Delta, *Glob. Change Biol.*, 21, 750-765, doi:10.1111/gcb.12745, 2015.

753 Koebisch, F., Glatzel, S., Hofmann, J., Forbrich, I. and Jurasinski, G.: CO<sub>2</sub> exchange of a temperate fen  
754 during the conversion from moderately rewetting to flooding, *J. Geophys. Res.-Biogeo.*, 118, 940-  
755 950, doi:10.1002/jgrg.20069, 2013.



756 Koebisch, F., Jurasinski, G., Koch, M., Hofmann, J. and Glatzel, S.: Controls for multi-scale temporal  
757 variation in ecosystem methane exchange during the growing season of a permanently inundated  
758 fen, *Agr. Forest Meteorol.*, 204, 94-105, doi:10.1016/j.agrformet.2015.02.002, 2015.

759 Kormann, R. and Meixner, F. X.: An analytical footprint model for non-neutral stratification, *Bound.-*  
760 *Lay. Meteorol.*, 99, 207-224, doi:10.1023/A:1018991015119, 2001.

761 Kortelainen, P., Rantakari, M., Huttunen, J. T., Mattsson, T., Alm, J., Juutinen, S., Larmola, T., Silvola, J.  
762 and Martikainen, P. J.: Sediment respiration and lake trophic state are important predictors of  
763 large CO<sub>2</sub> evasion from small boreal lakes, *Glob. Change Biol.*, 12, 1554-1567, doi: 10.1111/j.1365-  
764 2486.2006.01167.x. 2006.

765 Lamers, L. P. M., Vile, M. A., Grootjans, A. P., Acreman, M. C., van Diggelen, R., Evans, M. G., Richardson,  
766 C. J., Rochefort, L., Koojiman, A. M., Roelofs, J. G. M. and Smolders, A. J. P.: Ecological restoration  
767 of rich fens in Europe and North America: from trial and error to an evidence-based approach,  
768 *Biol. Rev.*, 90, 182-203, doi: 10.1111/brv.12102, 2015.

769 Lloyd, J. and Taylor, J. A.: On the temperature dependence of soil respiration, *Funct. Ecol.*, 8, 315-323,  
770 doi:10.2307/2389824, 1994.

771 Lund, M., Lafleur, P. M., Roulet, N. T., Lindroth, A., Christensen, T. R., Aurela, M., Chojnicki, B. H.,  
772 Flanagan, L. B., Humphreys, E. R., Laurila, T., Oechel, W., Olejnik, J., Rinne, J., Schubert, P. and  
773 Nilsson, M. B.: Variability in exchange of CO<sub>2</sub> across 12 northern peatland and tundra sites, *Glob.*  
774 *Change Biol.*, 16, 2436-2448, doi:10.1111/j.1365-2486.2009.02104.x, 2010.

775 MacIntyre, S., Jonsson, A., Jansson, M., Aberg, J., Turney, D. E. and Miller, S. D.: Buoyancy flux,  
776 turbulence, and the gas transfer coefficient in a stratified lake, *Geophys. Res. Lett.*, 37, L24604,  
777 doi:10.1029/2010GL044164, 2010.

778 Mauder, M. and Foken, T.: Documentation and instruction manual of the Eddy covariance software  
779 package TK2. Arbeitsergebnisse Nr. 26, University of Bayreuth, Department of Micrometeorology,  
780 42 pp, 2004.

781 McDermitt, D., Burba, G., Xu, L., Anderson, T., Komissarov, A., Riensche, B., Schedlbauer, J., Starr, G.,  
782 Zona, D., Oechel, W., Oberbauer, S. and Hastings, S.: A new low-power, open-path instrument for  
783 measuring methane flux by eddy covariance, *Appl. Phys. B*, 102, 391-405, doi:10.1007/s00340-  
784 010-4307-0, 2011.

785 Meyer, K., Höper, H. and Blankenburg, J.: Spurengashaushalt und Klimabilanz von Niedermooren unter  
786 dem Einfluß des Vernässungsmanagements, in: *Ökosystemmanagement für Niedermoore.*

787 Strategien und Verfahren zur Renaturierung, edited by Kratz, R. and Pfadenhauer, J., Ulmer,  
788 Stuttgart, 104-111, 2001.

789 Minke, M., Augustin, J., Burlo, A., Yarmashuk, T., Chuvashova, H., Thiele, A., Freibauer, A., Tikhonov, V.  
790 and Hoffmann, M.: Water level, vegetation composition and plant productivity explain  
791 greenhouse gas fluxes in temperate cutover fens after inundation, *Biogeosciences Discussions*,  
792 12, 17393-17452, doi:10.5194/bgd-12-17393-2015, 2015.

793 Moffat, A. M., Papale, D., Reichstein, M., Hollinger, D. Y., Richardson, A. D., Barr, A. G., Beckstein, C.,  
794 Braswell, B. H., Churkina, G., Desai, A. R., Falge, E., Gove, J. H., Heimann, M., Hui, D., Jarvis, A. J.,  
795 Kattge, J., Noormets, A. and Stauch, V. J.: Comprehensive comparison of gap-filling techniques for  
796 eddy covariance net carbon fluxes, *Agr. Forest Meteorol.*, 147, 209-232,  
797 doi:10.1016/j.agrformet.2007.08.011, 2007.

798 Moncrieff, J. B., Clement, R., Finnigan, J. and Meyers, T.: Averaging, detrending and filtering of eddy  
799 covariance time series, in: *Handbook of micrometeorology: a guide for surface flux*  
800 *measurements*, edited by Lee, X., Massman, W. J. and Law, B. E., Kluwer Academic, Dordrecht, 7-  
801 31, doi:10.1007/1-4020-2265-4, 2004.

802 Morrissey, L. A., Zobel, D. B. and Livingston, G. P.: Significance of stomatal control on methane release  
803 from *Carex*-dominated wetlands, *Chemosphere*, 26, 339-355, doi:10.1016/0045-6535(93)90430-  
804 D, 1993.

805 Naiman, R. J., Manning, T. and Johnston, C. A.: Beaver population fluctuations and tropospheric  
806 methane emissions in boreal wetlands, *Biogeochemistry*, 12, 1-15, doi: 10.1007/BF00002623,  
807 1991.

808 Nilsson, M., Mikkilä, C., Sundh, I., Granberg, G., Svensson, B. H. and Ranneby, B.: Methane emission  
809 from Swedish mires: National and regional budgets and dependence on mire vegetation, *J.*  
810 *Geophys. Res.*, 106, 20847-20860, doi:10.1029/2001JD900119, 2001.

811 Petrescu, A. M. R., Lohila, A., Tuovinen, J.-P., Baldocchi, D. D., Desai, A. R., Roulet, N. T., Vesala, T.,  
812 Dolman, A. J., Oechel, W. C., Marcolla, B., Friborg, T., Rinne, J., Hatala Matthes, J., Merbold, L.,  
813 Meijide, A., Kiely, G., Sottocornola, M., Sachs, T., Zona, D., Varlagin, A., Lai, D. Y. F., Veenendaal,  
814 E., Parmentier, F.-J. W., Skiba, U., Lund, M., Hensen, A., van Huissteden, J., Flanagan, L. B.,  
815 Shurpali, N. J., Grünwald, T., Humphreys, E. R., Jackowicz-Korczyński, M., Aurela, M. A., Laurila, T.,  
816 Grüning, C., Corradi, C. A. R., Schrier-Uijl, A. P., Christensen, T. R., Tamstorf, M. P., Mastepanov,  
817 M., Martikainen, P. J., Verma, S. B., Bernhofer, C. and Cescatti, A.: The uncertain climate footprint  
818 of wetlands under human pressure, *PNAS*, 112, 4594-4599, doi:10.1073/pnas.1416267112, 2015.

819 Podgrajsek, E., Sahlée, E. and Rutgersson, A.: Diurnal cycle of lake methane flux, *J. Geophys. Res.-*  
820 *Biogeo.*, 119, 236-248, doi:10.1002/2013JG002327, 2014.

821 Poindexter, C. M. and Variano, E. A.: Gas exchange in wetlands with emergent vegetation: the effects  
822 of wind and thermal convection at the air–water interface, *J. Geophys. Res.-Biogeo.*, 118, 1297–  
823 1306, doi:10.1002/jgrg.20099, 2013.

824 Poissant, L., Constant, P., Pilote, M., Canário, J., O’Driscoll, N., Ridal, J. and Lean, D.: The ebullition of  
825 hydrogen, carbon monoxide, methane, carbon dioxide and total gaseous mercury from the  
826 Cornwall Area of Concern, *Sci. Total Envir.*, 381, 256-262, doi:10.1016/j.scitotenv.2007.03.029,  
827 2007.

828 R Core Team: *R: A Language and Environment for Statistical Computing*. R Foundation for Statistical  
829 Computing, Vienna, Austria, 2012.

830 Read, J. S., Hamilton, D. P., Desai, A. R., Rose, K. C., MacIntyre, S., Lenters, J. D., Smyth, R. L., Hanson,  
831 P. C., Cole, J. J., Staehr, P. A., Rusak, J. A., Pierson, D. C., Brookes, J. D., Laas, A. and Wu, C. H.: Lake-  
832 size dependency of wind shear and convection as controls on gas exchange, *Geophys. Res. Lett.*,  
833 39, L09405, doi:10.1029/2012GL051886, 2012.

834 Reichstein, M., Falge, E., Baldocchi, D., Papale, D., Aubinet, M., Berbigier, P., Bernhofer, C., Buchmann,  
835 N., Gilmanov, T., Granier, A., Grünwald, T., Havránková, K., Ilvesniemi, H., Janous, D., Knohl, A.,  
836 Laurila, T., Lohila, A., Loustau, D., Matteucci, G., Meyers, T., Miglietta, F., Ourcival, J.-M.,  
837 Pumpanen, J., Rambal, S., Rotenberg, E., Sanz, M., Tenhunen, J., Seufert, G., Vaccari, F., Vesala, T.,  
838 Yakir, D. and Valentini, R.: On the separation of net ecosystem exchange into assimilation and  
839 ecosystem respiration: review and improved algorithm, *Glob. Change Biol.*, 11, 1424-1439,  
840 doi:10.1111/j.1365-2486.2005.001002.x, 2005.

841 Repo, M. E., Huttunen, J. T., Naumov, A. V., Chichulin, A. V., Lapshina, E. D., Bleuten, W. and  
842 Martikainen, P. J.: Release of CO<sub>2</sub> and CH<sub>4</sub> from small wetland lakes in western Siberia, *Tellus*, 59B,  
843 788-796, doi:10.1111/j.1600-0889.2007.00301.x, 2007.

844 Rinne, J., Riutta, T., Pihlatie, M., Aurela, M., Haapanala, S., Tuovinen, J.-P., Tuittila, E.-S. and Vesala, T.:  
845 Annual cycle of methane emission from a boreal fen measured by the eddy covariance technique,  
846 *Tellus*, 59B, 449-457, doi:10.1111/j.1600-0889.2007.00261.x, 2007.

847 Rocha, A. V. and Goulden, M. L.: Large interannual CO<sub>2</sub> and energy exchange variability in a freshwater  
848 marsh under consistent environmental conditions, *J. Geophys. Res.*, 113, G04019,  
849 doi:10.1029/2008JG000712, 2008.

850 Rõõm, E.-I., Nõges, P., Feldmann, T., Tuvikene, L., Kisand, A., Teearu, H. and Nõges, T.: Years are not  
851 brothers: Two-year comparison of greenhouse gas fluxes in large shallow Lake Võrtsjärv, Estonia,  
852 *J. Hydrol.*, 519, 1594-1606, doi:10.1016/j.jhydrol.2014.09.011, 2014.

853 Roulet, N. T., Ash, R. and Moore, T. R.: Low boreal wetlands as a source of atmospheric methane, *J.*  
854 *Geophys. Res.*, 97, 3739-3749, 1992.

855 Roulet, N.T., Ash, R., Quinton, W. and Moore, T. R.: Methane flux from drained northern peatlands:  
856 Effect of a persistent water table lowering on flux, *Global Biogeochem. Cy.*, 7, 749-769,  
857 doi:10.1029/93GB01931, 1993.

858 Sahlée, E., Rutgersson, A., Podgrajsek, E. and Bergström, H.: Influence from surrounding land on the  
859 turbulence measurements above a lake, *Bound.-Lay. Meteorol.*, 150, 235-258,  
860 doi:10.1007/s10546-013-9868-0, 2014.

861 Schrier-Uijl, A. P., Veraart, A. J., Leffelaar, P. A., Berendse, F. and Veenendaal, E. M.: Release of CO<sub>2</sub> and  
862 CH<sub>4</sub> from lakes and drainage ditches in temperate wetlands, *Biogeochemistry*, 102, 265-279,  
863 doi:10.1007/s10533-010-9440-7, 2011.

864 Schrier-Uijl, A. P., Kroon, P. S., Hendriks, D. M. D., Hensen, A., van Huissteden, J., Berendse, F. and  
865 Veenendaal, E. M.: Agricultural peatlands: towards a greenhouse gas sink – a synthesis of a  
866 Dutch landscape study, *Biogeosciences*, 11, 4559-4576, doi:10.5194/bg-11-4559-2014, 2014.

867 Sepulveda-Jauregui, A., Walter Anthony, K. M., Martinez-Cruz, K., Greene, S. and Thalasso, F.: Methane  
868 and carbon dioxide emissions from 40 lakes along a north-south latitudinal transect in Alaska,  
869 *Biogeosciences*, 12, 3197-3223, doi:10.5194/bg-12-3197-2015, 2015.

870 Shoemaker, W. B., Anderson, F., Barr, J. G., Graham, S. L. and Botkin, D. B.: Carbon exchange between  
871 the atmosphere and subtropical forested cypress and pine wetlands, *Biogeosciences*, 12, 2285-  
872 2300, doi:10.5194/bg-12-2285-2015, 2015.

873 Siebicke, L., Hunner, M. and Foken, T.: Aspects of CO<sub>2</sub> advection measurements, *Theor. Appl. Climatol.*,  
874 109, 109-131, doi:10.1007/s00704-011-0552-3, 2012.

875 Silvius, M., Joosten, H. and Opdam, S.: Peatlands and people, in: *Assessment on peatlands, biodiversity*  
876 *and climate change: Main Report*, edited by Parish, F., Sirin, A., Charman, D., Joosten, H.,  
877 Minayeva, T., Silvius, M. and Stringer, L., Global Environment Centre, Kuala Lumpur, and Wetlands  
878 International, Wageningen, 20-38, 2008.

879 Smith, L. K. and Lewis Jr., W. M.: Seasonality of methane emissions from five lakes and associated  
880 wetlands of the Colorado Rockies, *Global Biogeochem. Cy.*, 6, 323-338, 1992.

881 Spawn, S. A., Dunn, S. T., Fiske, G. J., Natali, S. M., Schade, J. D. and Zimov, N. S.: Summer methane  
882 ebullition from a headwater catchment in Northeastern Siberia, *Inland Waters*, 5, 224-230,  
883 doi:10.5268/IW-5.3.845, 2015.

884 Steffenhagen, P., Zak, D., Schulz, K., Timmermann, T. and Zerbe, S.: Biomass and nutrient stock of  
885 submersed and floating macrophytes in shallow lakes formed by rewetting of degraded fens,  
886 *Hydrobiologia*, 692, 99-109, doi:10.1007/s10750-011-0833-y, 2012.

887 Strachan, I. B., Nugent, K. A., Crombie, S. and Bonneville, M.-C.: Carbon dioxide and methane exchange  
888 at a cool-temperate freshwater marsh, *Environ. Res. Lett.*, 10, 065006, doi:10.1088/1748-  
889 9326/10/6/065006, 2015.

890 Succow, M.: Durchströmungsmoore, in: *Landschaftsökologische Moorkunde*, edited by Succow, M.  
891 and Joosten, H., Schweizerbart, Stuttgart, 463-470, 2001.

892 Torn, M. S. and Chapin III, F. S.: Environmental and biotic controls over methane flux from arctic tundra,  
893 *Chemosphere*, 26, 357-368, doi:10.1016/0045-6535(93)90431-4, 1993.

894 van Dijk, A., Moene, A. F. and de Bruin, H. A. R.: *The principles of surface flux physics: Theory, practice*  
895 *and description of the ECPack library*, Meteorology and Air Quality Group, Wageningen University,  
896 Wageningen, 98 pp, 2004.

897 Vickers, D. and Mahrt, L.: Quality control and flux sampling problems for tower and aircraft data, *J.*  
898 *Atmos. Ocean. Tech.*, 14, 512-526, 1997.

899 Waddington, J. M. and Day, S. M.: Methane emissions from a peatland following restoration, *J.*  
900 *Geophys. Res.*, 112, G03018, doi:10.1029/2007JG000400, 2007.

901 Wagner, W. and Pruß, A.: The IAPWS formulation 1995 for the thermodynamic properties of ordinary  
902 water substance for general and scientific use, *J. Phys. Chem. Ref. Data*, 31, 387-535, 2002.

903 Wang, H., Lu, J., Wang, W., Yang, L. and Yin, C.: Methane fluxes from the littoral zone of hyper eutrophic  
904 Taihu Lake China, *J. Geophys. Res.*, 111, D17109, doi:10.1029/2005JD006864, 2006.

905 Webb, E. K., Pearman, G. I. and Leuning, R.: Correction of flux measurements for density effects due  
906 to heat and water vapor transfer, *Q. J. Roy. Meteor. Soc.*, 106, 85-100,  
907 doi:10.1002/qj.49710644707, 1980.

908 Whiting, G. J. and Chanton, J. P.: Greenhouse carbon balance of wetlands: methane emission versus  
909 carbon sequestration, *Tellus*, 53B, 521-528, doi: 10.1034/j.1600-0889.2001.530501.x, 2001.

910 Wilczak, J. M., Oncley, S. P. and Stage, S. A.: Sonic anemometer tilt correction algorithms, *Bound.-Lay.*  
911 *Meteorol.*, 99, 127-150, doi:10.1023/A:1018966204465, 2001.

912 Wilson, D., Tuittila, E.-S., Alm, J., Laine, J., Farrell, E. P. and Byrne, K. A.: Carbon dioxide dynamics of a  
913 restored maritime peatland, *Ecoscience* 14, 71-80, doi: 10.2980/1195-  
914 6860(2007)14[71:CDDOAR]2.0.CO;2, 2007.

915 Wilson, D., Alm, J., Laine, J., Byrne, K. A., Farrell, E. P. and Tuittila, E.-S.: Rewetting of cutaway  
916 peatlands: are we re-creating hot plots of methane emissions?, *Restor. Ecol.*, 17, 796-806,  
917 doi:10.1111/j.1526-100X.2008.00416.x, 2008.

918 Yavitt, J. B., Angell, L. L., Fahey, T. J., Cirimo, C. P. and Driscoll, C. T.: Methane fluxes, concentrations,  
919 and production in two Adirondack beaver impoundments, *Limnol. Oceanogr.*, 37, 1057-1066,  
920 1992.

921 Zak, D., Gelbrecht, J., Wagner, C. and Steinberg, C. E. W.: Evaluation of phosphorus mobilisation  
922 potential in rewetted fens by an improved sequential chemical extraction procedure, *Eur. J. Soil.*  
923 *Sci.*, 59, 1191-1201, doi:10.1111/j.1365-2389.2008.01081.x, 2008.

924 Zak, D., Reuter, H., Augustin, J., Shatwell, T., Barth, M., Gelbrecht, J. and McInnes, R. J.: Changes of the  
925 CO<sub>2</sub> and CH<sub>4</sub> production potential of rewetted fens in the perspective of temporal vegetation  
926 shifts, *Biogeosciences*, 12, 2455-2468, doi:10.5194/bg-12-2455-2015, 2015.

927 Zerbe, S., Steffenhagen, P., Parakenings, K., Timmermann, T., Frick, A., Gelbrecht, J. and Zak, D.:  
928 Ecosystem service restoration after 10 years of rewetting peatlands in NE Germany, *Environ.*  
929 *Manage.*, 51, 1194-1209, doi:10.1007/s00267-013-0048-2, 2013.

930 Zhu, D., Chen, H., Zhu, Q., Wu, Y. and Wu, N.: High Carbon Dioxide Evasion from an Alpine Peatland  
931 Lake: The Central Role of Terrestrial Dissolved Organic Carbon Input, *Water Air Soil Poll.*, 223,  
932 2563-2569, doi:10.1007/s11270-011-1048-6, 2012.

933

934 Table 1: Data loss and final data coverage during the observation period. CO<sub>2</sub> and CH<sub>4</sub> flux data were  
 935 lost by power and instrument failure and maintenance as well as quality control and footprint analysis.

Filter criteria	Percentage of data [%]	
	CO <sub>2</sub>	CH <sub>4</sub>
Power and instrument failure, maintenance	15.0	46.4
Absence of sensor	-	11.2
QC 2	7.5	2.0
RSSI	-	2.1
u*	18.6	8.8
Unreasonably high fluxes	0.2	0.1
No footprint information/footprint > 20 % outside the AOI	13.2	6.5
<b>Final data coverage</b>	<b>45.5</b>	<b>22.9</b>

936

937 Table 2: Gapfilling model performance was estimated according to Moffat et al. (2007) with several  
 938 measures ( $n_{\text{CO}_2} = 6193$ ,  $n_{\text{CH}_4} = 3386$ , fluxes of best quality QC 0): the adjusted coefficient of  
 939 determination  $R^2_{\text{adj}}$  for phase correlation (significant in all cases,  $p\text{-value} < 2.2e^{-16}$ ), the absolute root  
 940 mean square index ( $\text{RMSE}_{\text{abs}}$ ) and the mean absolute error (MAE) for the magnitude and distribution  
 941 of individual errors, as well as the bias error (BE) for the bias of the annual sums.

<b>Method</b>	<b><math>R^2_{\text{adj}}</math></b>	<b><math>\text{RMSE}_{\text{abs}}</math></b> ( $\text{mg m}^{-2} 30\text{min}^{-1}$ )	<b>MAE</b> ( $\text{mg m}^{-2} 30\text{min}^{-1}$ )	<b>BE</b> ( $\text{g m}^{-2} \text{a}^{-1}$ )
MDS <sub>CO2nofoot</sub>	0.74	104.35	24.05	13.14
NLR <sub>CO2foot</sub>	0.66	119.10	27.51	-2.12
NLR <sub>CH4nofoot</sub>	0.79	1.36	0.83	-3.34
NLR <sub>CH4foot</sub>	0.81	1.28	0.78	-2.54

942



943 Table 3: Annual balances of CO<sub>2</sub> and CH<sub>4</sub> derived by different methods for the whole EC source area,  
 944 the area of interest (AOI) and the two surface types: MDS approach without footprint consideration  
 945 (MDS<sub>CO2nofoot</sub>), NLR approach without (NLR<sub>CH4nofoot</sub>) and with (NLR<sub>CH4foot</sub>, NLR<sub>CO2foot</sub>) footprint  
 946 consideration. Uncertainty was calculated as square root of the sum of squared random uncertainty  
 947 (measurement uncertainty) and gapfilling uncertainty.

Source area	Flux (g m <sup>-2</sup> a <sup>-1</sup> )	Method			
		CO <sub>2</sub>		CH <sub>4</sub>	
		MDS <sub>CO2nofoot</sub>	NLR <sub>CO2foot</sub>	NLR <sub>CH4nofoot</sub>	NLR <sub>CH4foot</sub>
Whole EC source area	NEE	524.5 ± 5.6	531.4 ± 13.0		
	GPP	-2380.5 ± 5.6	-2122.1 ± 16.7		
	R <sub>eco</sub>	2863.6 ± 5.6	2603.6 ± 8.4		
	CH <sub>4</sub>			40.5 ± 0.2	39.8 ± 0.2
AOI	NEE		843.5 ± 13.0		
	GPP		-3192.2 ± 16.7		
	R <sub>eco</sub>		4035.7 ± 8.4		
	CH <sub>4</sub>				21.8 ± 0.2
Emergent vegetation	NEE		750.3 ± 13.0		
	GPP		-4076.8 ± 16.7		
	R <sub>eco</sub>		4827.2 ± 8.4		
	CH <sub>4</sub>				13.2 ± 0.2
Open water	NEE		158.2 ± 13.0		
	GPP		-1021.5 ± 16.7		
	R <sub>eco</sub>		1179.7 ± 8.4		
	CH <sub>4</sub>				52.6 ± 0.2

948

949 Table 4: NEE and net CH<sub>4</sub> exchange at open water sites. The letters in parentheses indicate seasonal  
 950 (S; May to October) and annual (A) budgets. Positive water level indicates inundated conditions. GHG  
 951 flux measurement methods are denoted as: CH = chambers, CO = concentration profiles, TR = gas traps.

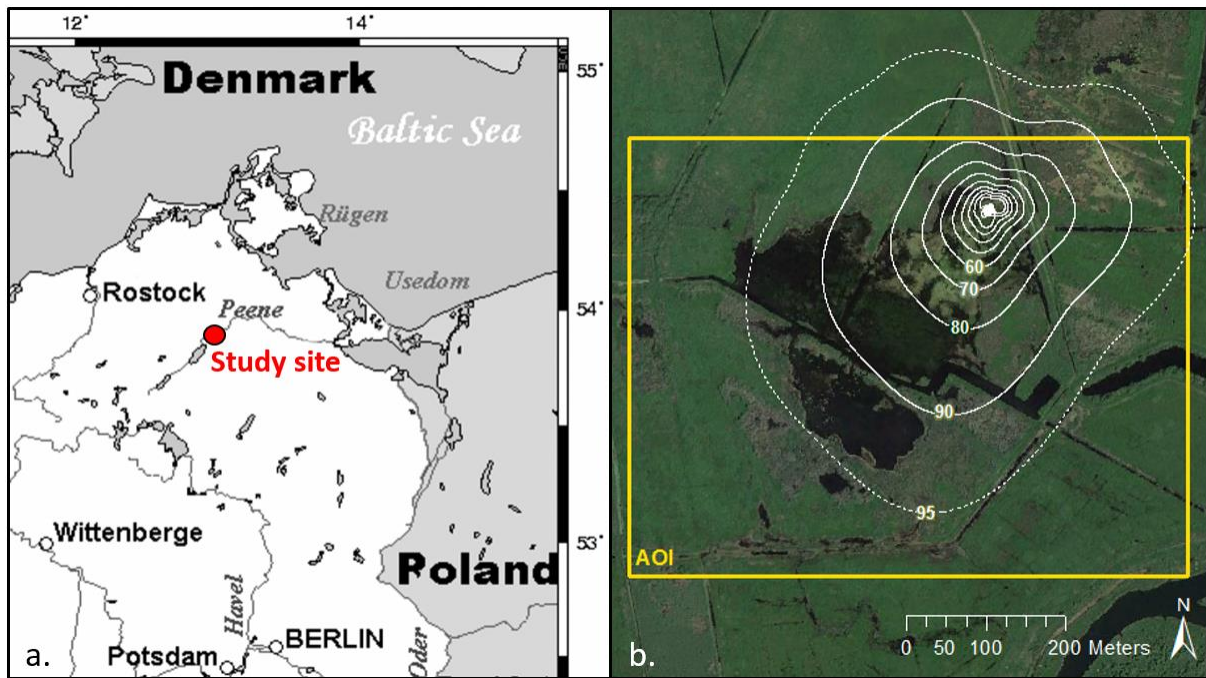
Reference	Location, ecosystem type	Dominant plant species	Study year	Average water depth (m)	NEE (g CO <sub>2</sub> m <sup>-2</sup> a <sup>-1</sup> )	CH <sub>4</sub> (g CH <sub>4</sub> m <sup>-2</sup> a <sup>-1</sup> )
Huttunen et al. (2003), CH	Lake Postilampi, Finland: hypertrophic lake		1997	3.2		16 (A)
Casper et al. (2000), TR/CO	Priest Pot, UK: hypertrophic lake		1997	2.3		13 (A)
Ducharme-Riel et al. (2015), CO	Bran-de-Scie, Quebec: eutrophic lake		2007-2008	3.2	224 (A)	
Wang et al. (2006), CH	Taihu Lake, China, hypertrophic lake: - bare infralittoral zone - pelagic zone		2003-2004	0.5 to 1.8 1.8		3 (A) 4 (A)
Hendriks et al. (2007), CH	Horstermeer, The Netherlands: eutrophic ditches		2005 2006	> 0 > 0		47 (A) 49 (A)
Waddington and Day (2007), CH	Bois-des-Bel peatland, Quebec: - ponds - ditches		2000-2002	> 0 > 0		0.3 (S) 2.9 (S)
Naimann et al. (1991), CH	Kabetogama Peninsula, Minnesota, beaver pond: - submergent aquatic plants - deep water	<i>Utricularia spp.</i> , <i>Potamogeton spp.</i>	1988	0.45 1.25		14 (A) 12 (A)
Roulet et al. (1992), CH	Low forest region, Ontario: beaver ponds		1990	0.2 to 0.4		7.6 (A)
Bubier et al. (1993), CH	Clay Belt, Ontario: beaver pond		1991	0.5 to 1.5		44 (A)
Yavitt et al. (1992), CH	New York, beaver ponds: - 3 years old - > 30 years old		1990	≤ 2 ≤ 2		34 (A) 40 (A)

952 Table 5: Annual (A)/seasonal (S) NEE, GPP,  $R_{eco}$  and net  $CH_4$  exchange at *Typha* sites. Positive water  
 953 level indicates inundated soil. GHG flux measurement methods are denoted as: CH = chambers, EC =  
 954 eddy covariance.

Reference	Location, ecosystem type	Dominant plant species	Study year	Mean water level (m)	NEE	GPP	$R_{eco}$	$CH_4$ (g $CH_4$ m <sup>-2</sup> a <sup>-1</sup> )
Kankaala et al. (2004), CH	Lake Vesijärvi, Finland: - inner cattail-reed zone	<i>Phragmites australis</i> , <i>Typha latifolia</i>	1997	< 0.1 to > 0.2				51 (S) <sup>1</sup>
			1998	< 0.1 to > 0.2				43 (S) <sup>1</sup> , 6 (S) <sup>2</sup>
Chu et al. (2015), EC	Lake Erie, Freshwater marsh	<i>Phragmites australis</i> , <i>Typha latifolia</i>	1997	< 0.1 to > 0.2				30 (S) <sup>1</sup>
			1998	< 0.1 to > 0.2				23 (S) <sup>1</sup> , 7 (S) <sup>2</sup>
			1999	< 0.1 to > 0.2				23 (S) <sup>1</sup>
			2011	0.3 to 0.6	-289 (A)	-3338 (A)	3049 (A)	58 (A)
Bonneville et al. (2008), EC Strachan et al. (2015), NEE: EC, CH4: CH	Mer Bleue, Canada, freshwater marsh	<i>Nymphaea odorata</i>	2012	0.3 to 0.6	109 (A)	-3490 (A)	3599 (A)	76 (A)
			2013	0.3 to 0.6	340 (A)	-2666 (A)	3006 (A)	70 (A)
			2005-2006 2005-2009	winter > summer ≈ 0	-967 (A) -462 to -1041 (A)	-3045 (A)	2078 (A)	170 (A)
Whiting and Chanton (2001), CH	Virginia, freshwater marsh	<i>Typha latifolia</i>	1992-1993	0.05 to 0.2	-3288 (A)			109 (A)
			1992 1993	0.05 to 0.2 0.05 to 0.2	-3587 (A) -4177 (A)			69 (A) 96 (A)
Rocha and Goulden (2008), EC	San Joaquin Freshwater Marsh Reserve, California: - freshwater marsh	<i>Typha latifolia</i>	1999 2000 2001 2012	winter +, midsummer - winter +, midsummer - winter +, midsummer - 1.07		-3994 (A) -6006 (A) -7717 (A)	4811 (A) 5980 (A) 6721 (A)	71 (A)
Knox et al. (2015), EC	- wetland (rewetted 2010)	<i>Schoenoplectus acutus</i> , <i>Typha</i> spp.	2012	0.26	-1455 (A)	-5519 (A)	4064 (A)	52 (A)
			2010	0.51	388 (A)			21 (A)
Petrescu et al. (2015), EC	- wetland (rewetted 2010)	?	2010	0.51	388 (A)			21 (A)
			2010-2011 2011-2012	0.13 < 0.13	553 (A) -414 (A)	-2825 (A) -3980 (A)	3375 (A) 3566 (A)	80 (A) 91 (A)
Minke et al. (2015), CH	Giel'cykau' kašyl, Belarus, fen (rewetted 1985)	<i>Typha latifolia</i> , <i>Hydrocharis morsus-ranae</i>	2011	0.02	-156 (A)			13 (A)
			2012	-0.09	345 (A)			4 (A)
Wilson et al. (2007, 2008), CH	Turraun, Ireland, cutover bog (rewetted 1991)	<i>Typha latifolia</i>	2002	0.07	975 (A)	-3272 (A)	4064 (A)	39 (A)
			2003	0.03	1653 (A)	-4357 (A)	6010 (A)	29 (A)

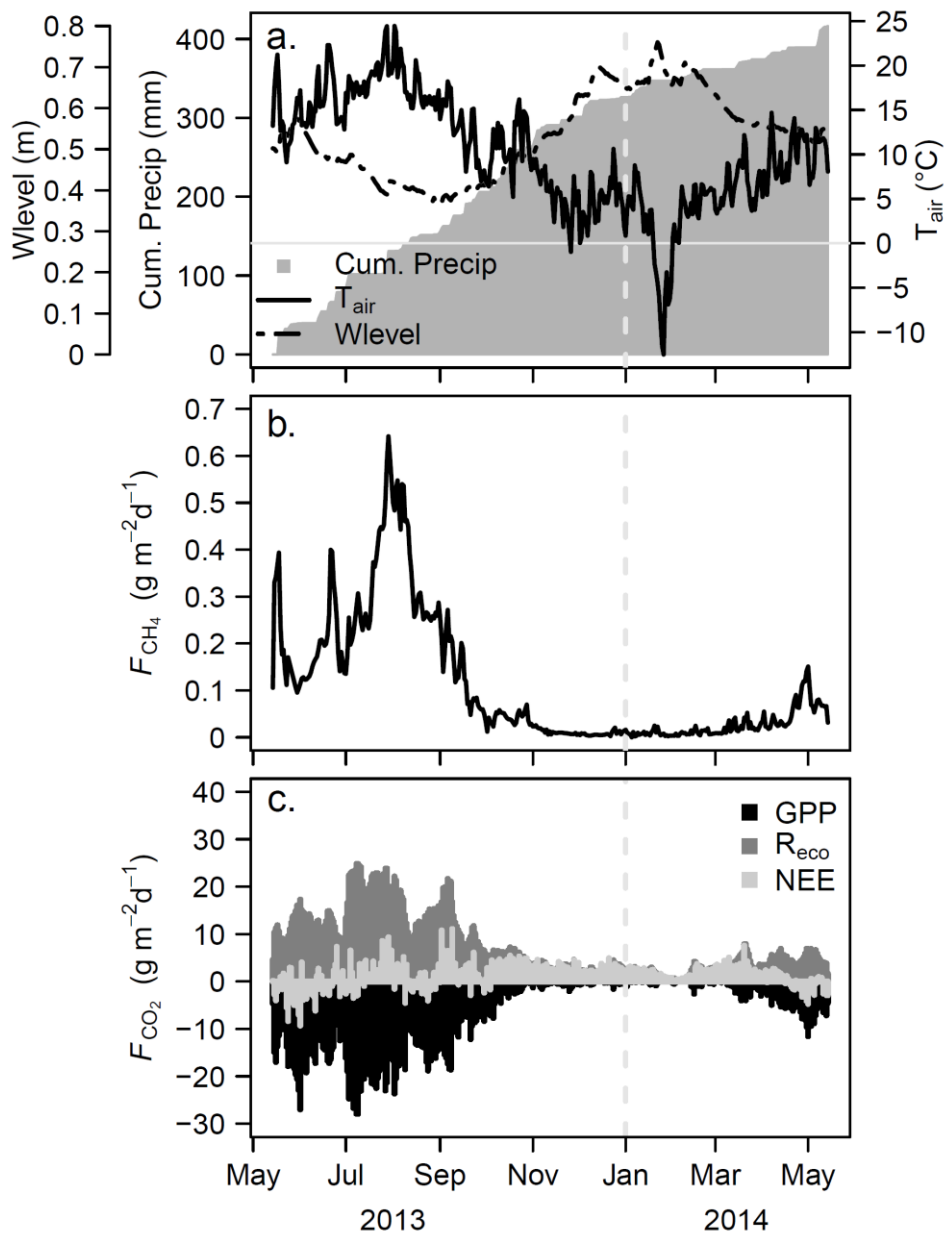
<sup>1</sup> open water period

<sup>2</sup> winter



955  
 956 Figure 1: a) Polder Zarnekow is situated in NE Germany within the Peene River valley; map source and  
 957 copyright: <https://commons.wikimedia.org/wiki/File:Germanymap2.png> (modified). b) Footprint  
 958 climatology calculated according to Chen et al. (2011) on a Landsat image (6 Jun 2013, source: Google  
 959 Earth). White lines represent the isopleths of the cumulative annual footprint climatology, where the  
 960 area within the 95 isopleth indicates 95 % contribution to the annual flux. The white dot denotes the  
 961 tower position. The yellow box indicates the area of interest (AOI) as a filter criterion to focus on fluxes  
 962 of the shallow lake and to avoid the possible impact of a farm and grassland to the north of the shallow  
 963 lake. If the half-hourly flux source area exceeded the AOI by more than 20 % the flux was discarded.  
 964 The site is characterised by two main surface types: open water and emergent vegetation.

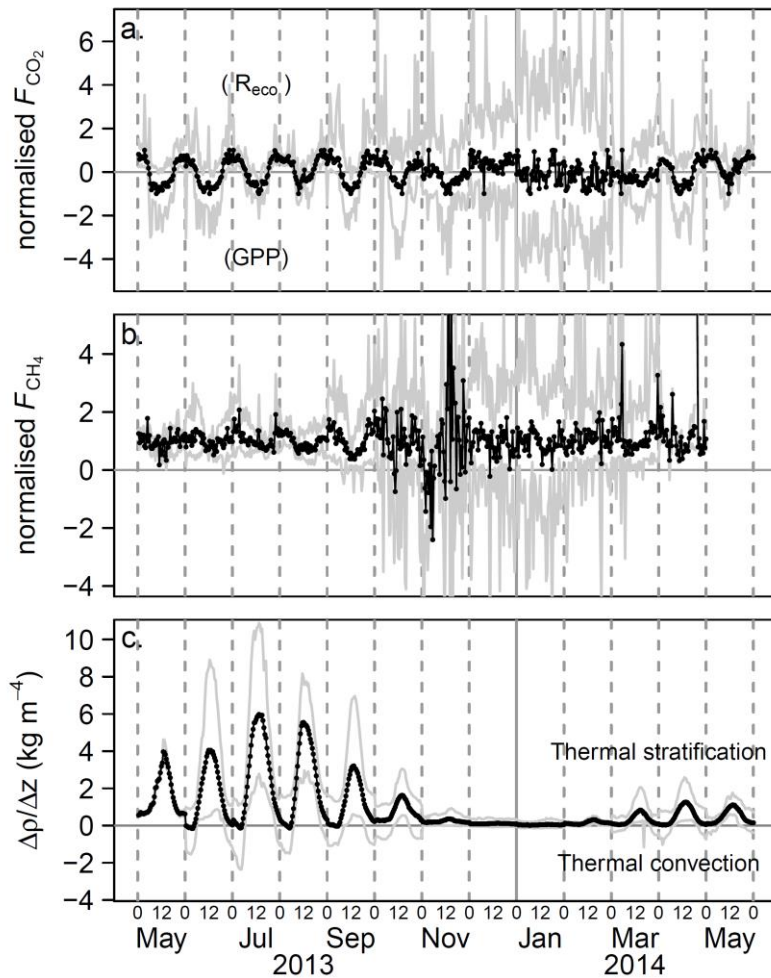
965



966

967 Figure 2: Temporal variability of environmental variables and ecosystem CO<sub>2</sub> and CH<sub>4</sub> exchange within  
 968 the EC source area. Seasonal course a) of water level (Wlevel), cumulative precipitation (Cum. Precip)  
 969 and air temperature (T<sub>air</sub>), b) the daily CH<sub>4</sub> flux (gapfilled, NLR<sub>CH<sub>4</sub>nofoot</sub>) and c) the daily NEE (gapfilled  
 970 MDS<sub>CO<sub>2</sub>nofoot</sub>) and component fluxes (modelled R<sub>eco</sub> and GPP, MDS<sub>CO<sub>2</sub>nofoot</sub>).

971



972

973 Figure 3: Average diurnal cycle of a) CO<sub>2</sub> flux, b) CH<sub>4</sub> flux and c) the water density gradient per month.

974 The numbers at the x-axis denote midnight (0) and midday (12) in UTC. Midnight is also illustrated with

975 a dashed line. Black and grey lines represent the mean and the range, respectively. The CO<sub>2</sub> and CH<sub>4</sub>

976 fluxes are normalised with the monthly minimum/ maximum and the median of the half-hourly fluxes,

977 respectively. Although the zero line is slightly shifted due to normalisation, positive CO<sub>2</sub> fluxes roughly

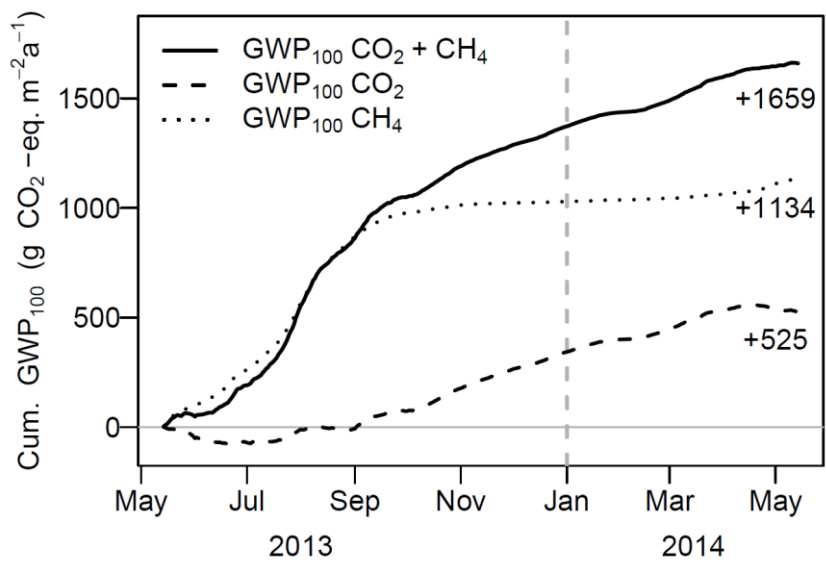
978 indicate the dominance of R<sub>eco</sub> against GPP, negative fluxes the dominance of GPP against R<sub>eco</sub>. The

979 period of ice-cover was excluded from the calculation of the temperature gradient. A density gradient

980 equal to or below zero indicates thermally induced convective mixing down to the bottom of the open

981 water body of the shallow lake, positive gradients instead thermal stratification.

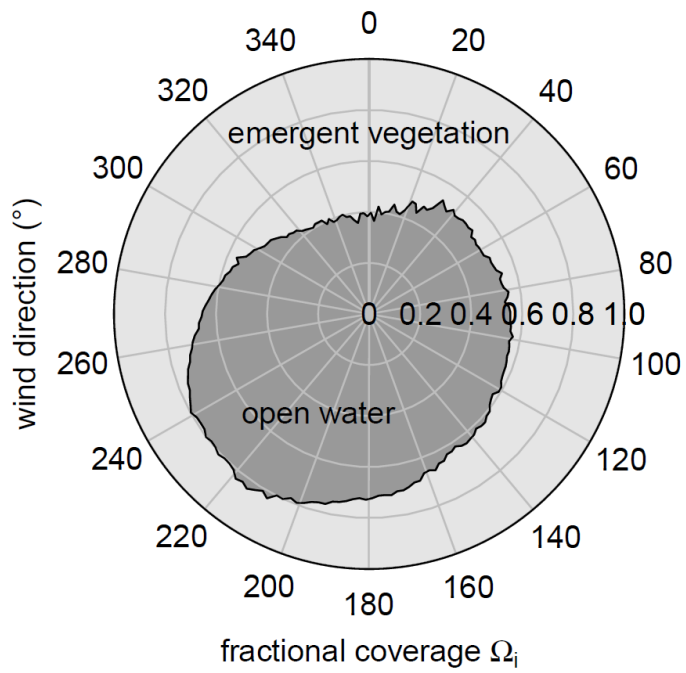
982



983

984 Figure 4: Cumulative GWP<sub>100</sub> budgets of CO<sub>2</sub> (based on MDS<sub>CO2nofoot</sub>), CH<sub>4</sub> (based on NLR<sub>CH4nofoot</sub>) and  
 985 the sum of both for the EC source area during the observation period.

986

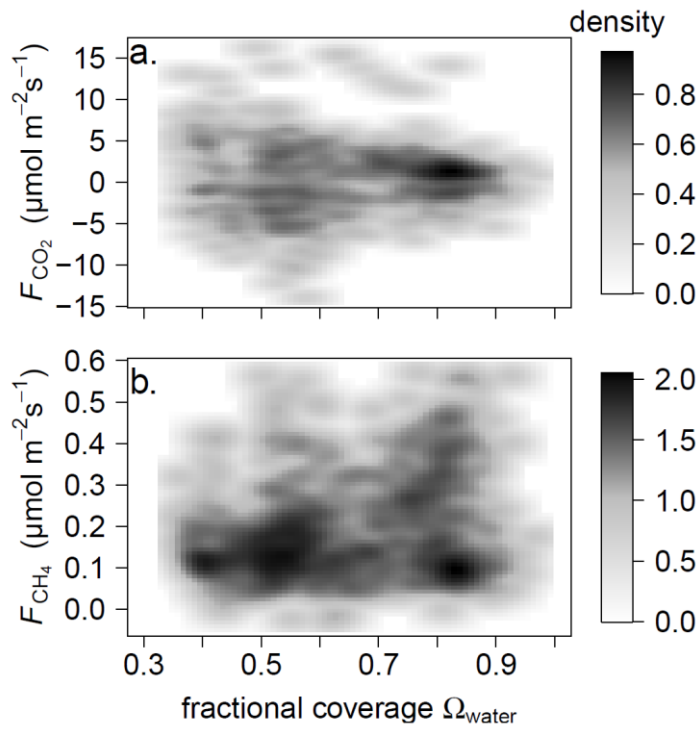


987

988 Figure 5: Source area fraction  $\Omega_i$  of the two main surface types in dependence on the wind direction  
 989 ( $2^\circ$ -bins).

990

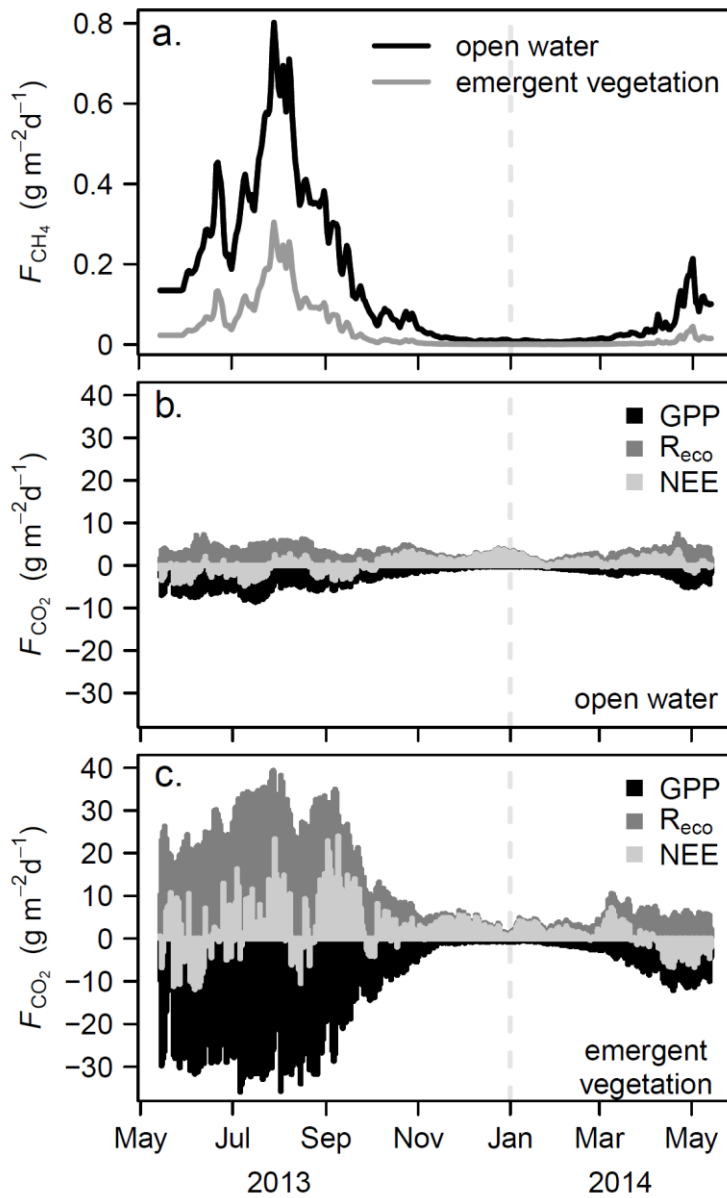




991

992 Figure 6: Impact of the fractional coverage of open water ( $\Omega_{\text{water}}$ ) within the EC source area on the  
 993 measured fluxes of  $\text{CO}_2$  and  $\text{CH}_4$  (15 May to 14 September 2013). The abundances of  $\text{CO}_2$  and  $\text{CH}_4$  fluxes  
 994 in dependence on  $\Omega_{\text{water}}$  are illustrated by a smoothed two-dimensional kernel density estimate. The  
 995 variability of  $\text{CO}_2$  flux rates decreased with increasing  $\Omega_{\text{water}}$ , whereas the variability of the  $\text{CH}_4$  flux  
 996 increased.

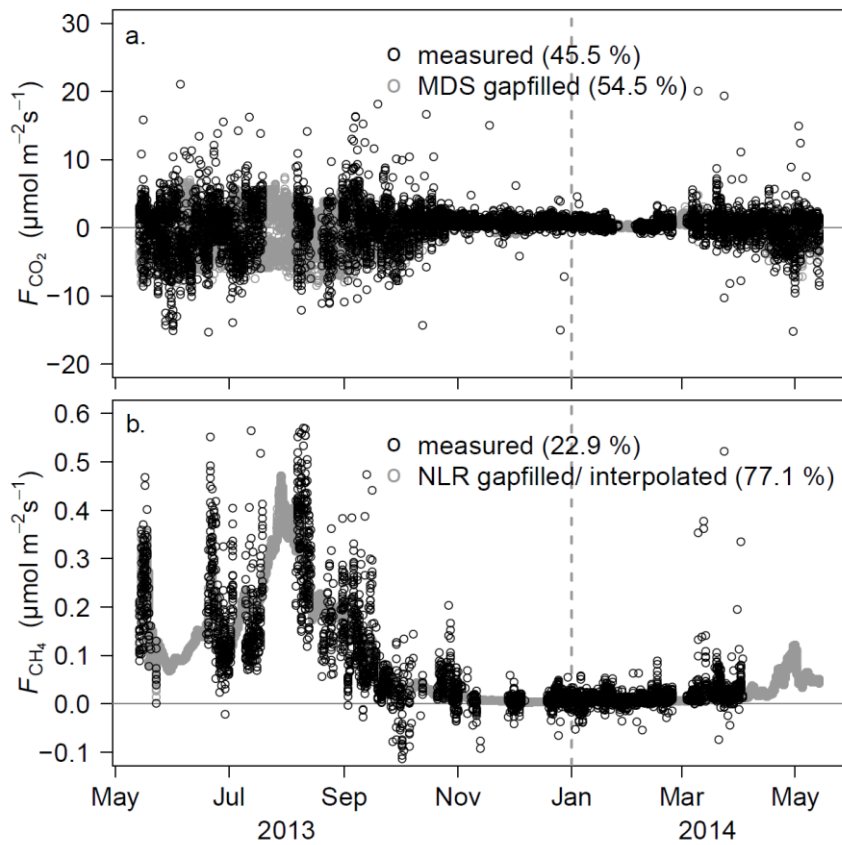
997



998

999 Figure 7: Daily CH<sub>4</sub>, NEE and component fluxes ( $R_{eco}$  and GPP) for the surface types: a) daily CH<sub>4</sub> flux of  
 1000 open water and emergent vegetation, b) daily NEE and component fluxes for open water, c) daily NEE  
 1001 and component fluxes for emergent vegetation, derived by NLR with the source area fractions of the  
 1002 surface types ( $\Omega_i$ ) as weighting factors ( $NLR_{CH_4foot}$ ,  $NLR_{CO_2foot}$ ).

1003



1004

1005 Figure A1: Measurement coverage of a) CO<sub>2</sub> and b) CH<sub>4</sub> fluxes within the study period. Gapfilling results  
 1006 of the MDS<sub>CO<sub>2</sub>nofoot</sub> and NLR<sub>CH<sub>4</sub>nofoot</sub> approaches are added as grey circles. The percentages in brackets  
 1007 indicate the time series coverages of measurements and gapfilling values.

1008